CASE FILE
COPY

NACA TN 2611

NATIONAL ADVISORY COMMITTEE FOR AERONAUTICS

TECHNICAL NOTE 2611

EXPERIMENTAL INVESTIGATION OF BASE PRESSURE ON BLUNT-TRAILING-EDGE WINGS AT SUPERSONIC VELOCITIES

By Dean R. Chapman, William R. Wimbrow,
and Robert H. Kester

Ames Aeronautical Laboratory
Moffett Field, Calif.

Washington
January 1952

1Q

NATIONAL ADVISORY COMMITTEE FOR AERONAUTICS

TECHNICAL NOTE 2611

EXPERIMENTAL INVESTIGATION OF BASE PRESSURE ON BLUNT-TRAILING-EDGE WINGS AT SUPERSONIC VELOCITIES

By Dean R. Chapman, William R. Wimbrow,
and Robert H. Kester

SUMMARY

Measurements of base pressure are presented for 29 blunt-trailing-edge wings having an aspect ratio of 3.0 and various airfoil profiles. The different profiles comprised thickness ratios between 0.05 and 0.10, boattail angles between -2.9° and 20°, and ratios of trailing-edge thickness to airfoil thickness between 0.2 and 1.0. The tests were conducted at Mach numbers of 1.25, 1.5, 2.0, and 3.1. For each Mach number, the Reynolds number and angle of attack were varied. The lowest Reynolds number investigated was 0.2×10^{6} and the highest was 3.5×10^{6}. Measurements on each wing were obtained separately with turbulent flow and laminar flow in the boundary layer. Spanwise surveys of the base pressure were conducted on several wings.

The results with turbulent boundary-layer flow showed only small effects on base pressure of variations in Reynolds number, airfoil profile shape, boattail angle, and angle of attack. The principal variables affecting the base pressure for turbulent flow were Mach number and the ratio of boundary-layer thickness to trailing-edge thickness.

The results obtained with laminar boundary-layer flow to the trailing edge showed that the effect of Reynolds number on base pressure was large. In all but a few exceptional cases the effects on base pressure of variations in profile shape, boattail angle, and angle of attack were appreciable though not large. The principal variable affecting the base pressure for laminar flow was the ratio of boundary-layer thickness to trailing-edge thickness.

For a few exceptional cases involving laminar flow to the trailing edge, the effects on base pressure of variations in profile shape, boattail angle, and angle of attack were found to be unusually large. In such cases the variation of base pressure with angle of attack was

discontinuous and exhibited a hysteresis. Stroboscopic schlieren observations at a Mach number of 1.5 revealed that these apparently special phenomena were associated with a vortex trail of relatively high frequency.

INTRODUCTION

In comparison to the numerous base pressure investigations conducted in the past on bodies of revolution, there have been relatively few such investigations conducted on two-dimensional airfoils. Some measurements of base pressure on wedge-type profiles have been reported in references 1, 2, and 3. These existing data, however, are inadequate for engineering purposes. Without considerable experimental information on base pressure, the base drag cannot be estimated for a given airfoil profile at given flight conditions.

Recently interest has developed in blunt-trailing-edge airfoils because of certain structural and aerodynamic advantages at high flight velocities. In particular, it has been found that at supersonic velocities a properly designed blunt-trailing-edge airfoil can have less drag and a greater lift-curve slope than a sharp-trailing-edge airfoil having the same strength or stiffness. A method of determining the airfoil profile having the least possible pressure drag has been developed in reference 4, but this method requires a knowledge of the base pressure for any given set of design flight conditions. Since the available base pressure data are meager, the purpose of the present investigation was to obtain information on the effects of Mach number, Reynolds number, type of boundary-layer flow, and airfoil profile shape on the base pressure of blunt-trailing-edge wings. Quantitative information on these effects is particularly important at low and moderate supersonic velocities because the base drag at these velocities can contribute the major portion of the total profile drag. The base drag of a 5-percent-thick wedge airfoil at a Mach number of 1.5, for example, amounts to approximately three-fourths of the total profile drag.

NOTATION

c airfoil chord

f vortex frequency

h trailing-edge thickness

p static pressure

M Mach number

Re Reynolds number

t maximum airfoil thickness

V velocity

α angle of attack

β boattail angle

δ boundary-layer thickness

φ trailing-edge bevel angle, measured between trailing-edge plane and plane normal to chord

Subscripts

b base

∞ free stream

Special Notation

(R) denotes rounded ridge lines when added either after the identification number of a wing, or after a symbol in a figure legend

APPARATUS AND TEST METHODS

Wind Tunnels

The experimental investigation was conducted in the Ames 1- by 3-foot supersonic wind tunnels No. 1 and No. 2. The No. 1 wind tunnel is of the closed-circuit, continuous-operation type and is equipped with a flexible-plate nozzle that provides a variation of Mach number from 1.2 to 2.2. The total pressure in the tunnel can be varied to provide Reynolds numbers from 0.2 to 1.7 million based on the 3-inch chord of the models employed in this investigation. The No. 2 wind tunnel is of the nonreturn, intermittent-operation type and is also equipped with a flexible-plate nozzle that provides a variation of Mach number from 1.2 to 4.0. The reservoir pressure can be varied to provide a variation in Reynolds number.

The water content of the air in both the 1- by 3-foot wind tunnels is maintained at less than 0.0003 pound of water per pound of dry air; consequently, the effect of humidity on the flow is negligible.

Models

Fifty-five wings with rectangular plan forms and blunt trailing edges were employed in this investigation. Data are presented for 29 of these wings; the others exhibited the same properties as the wings for which data are presented. All these wings were made of steel with a span of 9 inches and a chord of 3 inches. Originally each had an orifice located in the blunt trailing edge 3-1/2 inches inboard from one wing tip for measuring the base pressure. During the course of the investigation it was found to be desirable to relocate each orifice to a position 2-1/4 inches inboard from the wing tip (approximate center of exposed semispan). The first orifice position investigated is referred to as the "inboard" orifice position, and the relocated position is referred to as the "center" orifice position.

Most of the wings may be divided into two groups according to the purpose for which they were intended. One group was employed to investigate the effects of airfoil thickness ratio t/c and trailing-edge thickness ratio h/t on the base pressure. The profiles, dimensions, and the method of identifying these wings are shown in part A of table I. They are hereafter referred to as the "thickness group." The ridge lines on three of these wings were rounded during the course of the investigation. In the figures, wings with rounded ridge lines are designated by "(R)" after the wing identification number.

The second group of wings was employed to investigate the variation of base pressure with the boattail angle β. The profiles, dimensions, and identifying symbols of wings in this group are shown in part B of table I. They will be referred to as the "boattail group."

The surfaces of all the wings were originally ground and polished to approximately a 10-microinch root-mean-square surface. However, during the course of the investigation the wings became scratched from handling and from small foreign particles in the wind tunnels. In addition, all the wings were modified at least once during the investigation. From time to time various wings were polished to restore the surface finish to approximately its original smoothness. However, it was obvious that all the tests were not made on wings with the same degree of surface finish. Consequently, near the end of the investigation the surface roughness of all the wings was measured. Selected segments of the resulting trace records are shown in figure 1. The trace shown in figure 1(a) is typical of most of the surface of all the wings. That

shown in figure 1(b) is the roughest local segment of surface found on any wing. The trace shown in figure 1(c) is typical of the random scratches that were found on many of the wings.

Test Methods

Wing supports.- During the course of the investigation, three types of wing support were employed. The support adopted during the initial stages of the investigation was the sting-type support shown in figure 2(a). This support was designed from the viewpoint of minimum interference, but it proved to be too weak for the starting loads in the No. 2 wind tunnel. A stronger support was then adopted which utilized a 25-caliber ogive-cylinder body. This body was provided with two interchangeable nose sections of different lengths so that the effect of the position of the bow wave relative to the wing could be observed. The shorter length support is termed the "short body No. 1" (fig. 2(b)), and the longer length support is termed the "long body No. 1." The diameter of each body was 0.75 inch, and the nose was located 5-1/2 and 12 diameters, respectively, upstream of the wing leading edge. Unfortunately, this type of support also proved to be too weak and a fatigue failure of the afterbody occurred after considerable data had been obtained. The design of this support was then modified by enlarging the diameter of the afterbody as shown in figures 2(c) and 2(d). The resulting supports are referred to as the "short body No. 2" and "long body No. 2." For most of the data the short body No. 2 was employed. A comparison of base pressure measurements taken with the various supports is presented in appendix A. The particular support and orifice position used in obtaining the data presented in each figure of this report is listed at the end of appendix A.

Spanwise survey tube.- The spanwise variation of base pressure was measured on several wings of the thickness group with the survey tube shown in figure 2(b). The glass window on one side of the wind tunnel was replaced by a steel plate through which a 0.030-inch-diameter steel tube was passed. This tube was alined with a groove milled across the blunt trailing edge of the wing in a spanwise direction. To minimize interference with the flow about the wing, the survey tube passed through the support body and all measurements were made along the semispan of the wing opposite the side on which the survey tube entered the wind tunnel.

China-clay technique.- The china-clay technique suggested by Richards and Burstall (reference 5) and adapted to supersonic wind-tunnel testing by Gazley (reference 6) was used to indicate the state of the boundary-layer flow. Basically, the technique employed was as follows: The surfaces of the wings were sprayed with china clay suspended in a glyptol lacquer to give a thin, uniform coating. After drying, and just before the wings were installed in the wind tunnel, a

wetting agent with a slow rate of evaporation and approximately the same index of refraction as china clay was sprayed over the surfaces. This wetting agent makes the china clay coating transparent. When the wind tunnel is operated, the wetting agent evaporates at a higher rate in regions where turbulent flow exists than in laminar regions. At some time during this process the china-clay lacquer dries completely in the turbulent regions and appears white, while in the laminar regions the lacquer remains wet (except near the leading edge) and transparent.

The operating conditions of the two wind tunnels impose two entirely different sets of requirements on the properties of the wetting agent. In the No. 1 wind tunnel, the wetting agent must remain wet while the pressure is reduced to approximately 3 pounds per square inch absolute, the tunnel started, and the pressure brought back up to the level selected for the tests. The time required for this process is approximately 20 to 30 minutes. Upon reaching the desired pressure level, the tunnel may be operated for as long as is necessary for the transition pattern to appear. In contrast, the No. 2 tunnel starts almost instantaneously, requires just a few seconds to adjust to the desired pressure level, and can be operated for a very limited time. In addition, it was found that the stagnation temperature was so low in the No. 2 tunnel that some wetting agents tended to freeze after approximately 4 minutes of operation. After considerable experimenting it was found that eugenol was a satisfactory wetting agent in the No. 1 wind tunnel and that a mixture of half eugenol and half safrole gave the desired results in the No. 2 wind tunnel.

Typical photographs of wings on which the china clay was applied to smooth surfaces are shown in figure 3. The flow is from left to right in these photographs. It is seen that the boundary layer was laminar except in regions near the wing tip, and in the region near the wing-support juncture where transverse contamination presumably occurs. Also, the boundary layer turned turbulent behind particles that occasionally were lodged in the china clay. (See fig. 3(a).) For a Mach number of 3.1 an additional region of disturbance existed near the intersection of the wing and the body bow wave. This intersection occurred near the center of the exposed semispan for the short body support (fig. 3(d)), and near the wing tip for the long body support (fig. 3(c)). Similar photographs of wings with a boundary-layer trip added show that the boundary layer turned turbulent a short distance downstream of the trip. (See fig. 4.)

Boundary-layer trips.- As indicated by the china-clay photographs, it was necessary to use a boundary-layer trip in order to induce transition well ahead of the trailing edge. Photographs of three types of trips employed are shown in figure 5, and a discussion of the results obtained with each trip is presented in appendix B. For present purposes it will suffice to state that each trip effected transition satisfactorily, and that the corresponding base pressure measurements did not depend appreciably on the particular trip employed.

Procedure.- The variation with Reynolds number of the pressure acting on the blunt trailing edge of each wing was measured at nominal Mach numbers of 1.5 and 2.0 in the No. 1 wind tunnel. Selected wings were also tested at nominal Mach numbers of 1.5, 2.0, and 3.1 in the No. 2 wind tunnel. These base pressures were measured relative to the static pressure at reference orifices in the wind-tunnel walls. Calibration runs were also made at each Mach number to determine the local tunnel-empty static pressure at the station normally occupied by the trailing edge of the wings relative to these reference orifices. All the data are presented as the ratio of the base pressure to this local tunnel-empty static pressure.

Supplementary Apparatus for Schlieren Observations

The supports previously described made it impossible to observe the wake behind the blunt-trailing-edge wings through a schlieren apparatus. A two-dimensional channel provided a means of observing the flow in the vicinity of the trailing edge. The channel (shown in fig. 6) consisted essentially of two vertical flat plates between which airfoil models could be mounted horizontally. The plates were suspended in the test section of the wind tunnel in such a manner that the boundary layer on each side wall of the tunnel passed between the plate and the tunnel wall. The models were mounted between turntables in the plates so that the angle of attack could be varied. Optical glass windows were provided in these turntables and in the wind-tunnel walls.

The schlieren equipment consisted of a standard system for visual observation, a unit for flash photography, and a self-synchronizing stroboscopic schlieren unit similar to that described in reference 7. This latter unit will make any periodic fluctuations in the flow field covered by the schlieren apparatus appear stationary if the frequency is less than about 1,600 cycles per second. A photoelectric cell pick-up contained in this unit responds to fluctuations up to 80,000 cycles per second, and, therefore, an oscilloscope was employed in conjunction with this unit so that frequencies above 1,600 cycles could be measured, although not "stopped" on the schlieren viewing screen.

RESULTS AND DISCUSSION

Since previous measurements on bodies of revolution have shown a marked difference between the base pressure characteristics for turbulent flow in the boundary layer as compared to laminar flow, it might be expected that a similar difference also would exist on blunt-trailing-edge wings. It will become evident subsequently that this is the case. Because of such differences, it is advantageous to present and discuss the results obtained with turbulent flow separately from the results obtained with laminar flow.

Results Obtained With Boundary-Layer Trip on Wing Surfaces (Turbulent Boundary Layer)

Spanwise variation of base pressure for turbulent flow.- Inasmuch as the present measurements were made on finite-span wings, it is necessary to determine the spanwise variation of base pressure in order to estimate the degree to which the individual pressure measurements represent the actual base drag of a given wing. By using the survey tube described earlier, the base pressure was measured at various positions along one semispan on several wings of the thickness group at Mach numbers of 1.5 and 2.0. The results, presented in figure 7, show a large variation of base pressure in the vicinity of the tip, and a smaller variation inboard of the tip region. The large variations near the tip are believed to be associated with vortices. Observations on wing 10-1.00 with the vapor-screen technique (described by Allen and Perkins in reference 8) indicated that at zero lift two small vortices were shed near the tip corners of the trailing edge. These two vortices were located in a plane perpendicular to the chord plane and parallel to the free-stream direction. The variation of base pressure observed in several cases at extreme inboard locations is believed to be associated primarily with the disturbance to the boundary-layer flow originating at the wing-body juncture. Because of the large variations near the tip, it might be expected that spanwise variations of base pressure for low-aspect-ratio wings would preclude an accurate estimate of the base drag from measurements of base pressure at one spanwise station.

Correlation of data for the thickness group with turbulent flow.- A plot of the ratio p_b/p_∞ against the parameter $c/[h(Re)^{1/5}]$ is presented in figure 8 for the 12 wings of the thickness group. This parameter is approximately proportional to the ratio of turbulent boundary-layer thickness to trailing-edge thickness. The data for $M_\infty = 1.5$ and $M_\infty = 2.0$ were taken in the No. 1 wind tunnel at a Reynolds number of 1.7×10^6, and the data for $M_\infty = 3.1$ were taken in the No. 2 wind tunnel at a Reynolds number of 2.6×10^6. For each Mach number the scatter of the measurements representing the base pressure for turbulent flow is sufficiently small so that with reasonable accuracy a single correlation curve can be drawn through the data for all wings of this group.

At Mach numbers of 1.5 and 2.0 it was possible to test many of the wings of the thickness group in both wind tunnels. Figure 9 shows a comparison of the faired curves for $M_\infty = 1.5$ and $M_\infty = 2.0$ which represent the measurements described above with similar measurements obtained at higher Reynolds numbers in the No. 2 wind tunnel. It appears that the correlation curves determined from tests with a trip at $Re = 1.7 \times 10^6$ also apply at least up to the highest Reynolds numbers of the present tests. In addition, it is seen from figure 9(b) that the correlation curve for $M_\infty = 2.0$ applies with fair accuracy to the data obtained without a trip at a Reynolds number of 3.5×10^6. In this case natural

transition evidently occurs somewhere along the smooth surface upstream of the trailing edge.

The small difference between the measurements taken at $Re = 3.5 \times 10^6$ with and without a boundary-layer trip, and also the small slopes of the correlation curves for $M_\infty = 1.5$ and $M_\infty = 2.0$, indicate that the effect of Reynolds number on base pressure is small for turbulent boundary-layer flow. The sizable slope of the correlation curve for $M_\infty = 3.1$ also indicates that the effect of Reynolds number is relatively small since the abscissa involves the fifth root of the Reynolds number. The fact that at a given Mach number one correlation curve applies to all wings of the thickness group indicates that for a given boundary-layer thickness and trailing-edge thickness the base pressure is insensitive to moderate changes in profile shape upstream of the trailing edge.

Effect of boattail angle for turbulent flow.- Since the variations in profile shape between the different wings of the thickness group are not large, it was thought desirable to measure the base pressure on a separate group of wings comprising large variations in profile shape, particularly in boattail angle. The boattail group of wings was used for this purpose as this group contains three sets of profiles with a fixed trailing-edge thickness but with boattail angles ranging from 0° to 20°. A plot of base pressure against boattail angle is shown in figure 10. Included in this figure are several measurements from the thickness group plotted at their respective boattail angles. The effect of boattail angle on base pressure for the cases investigated is seen to be small for turbulent boundary-layer flow.

Effect of angle of attack for turbulent flow.- All measurements described up to this point were taken with the wings set at zero angle of attack. A plot of the base pressure against angle of attack for a number of wings of the thickness group is presented in figure 11. At Mach numbers of 1.5 and 3.1 there is seen to be only small effects of angle of attack on the base pressure within the angle range up to 5°. Similar results were found at a Mach number of 2.0.

Results Obtained With Smooth Surfaces (Laminar Boundary Layer)

Spanwise variation of base pressure for laminar flow.- The results of a spanwise survey of base pressure on two wings tested with smooth surfaces at $M_\infty = 1.5$ are presented in figure 12. On wing 10-1.00 the base pressure near the wing tip varies in much the same manner as for the case of turbulent boundary-layer flow (fig. 7). Over the midportion and inboard portion of the semispan, however, the base pressure is nearly constant. On wing 5-0.50(R), which has a relatively thin trailing edge, base pressure variations near the tip are confined to a smaller portion of the span than on wing 10-1.00, but additional small variations appear

near the wing-body juncture which are believed to be due to transverse contamination. (See, for example, the china-clay photograph in fig. 3(b).) In view of these results, measurements of base pressure presented in the section which follows were taken with an orifice located at the center of the exposed semispan. Some similar measurements with the inboard orifice are presented in appendix A.

Correlation of data of thickness group for laminar flow.- A plot of base pressure against the parameter $c/[h(Re)^{1/2}]$ which is approximately proportional to the ratio of laminar boundary-layer thickness to trailing-edge thickness, is shown in figure 13 for various wings of the thickness group tested with smooth surfaces at $M_\infty = 3.1$. These data were obtained at $Re = 2.0 \times 10^6$ and are believed to represent laminar flow to the trailing edge in view of the china-clay indications. At this Reynolds number, however, transition may be occurring in the wake close to the trailing edge. The few measurements taken at this Mach number show a considerable increase in base pressure as δ/h increases.

At $M_\infty = 2.0$ measurements were taken on all wings of the thickness group in the range of Reynolds number between 0.2×10^6 and 1.7×10^6. The results for the three thickness ratios investigated are plotted in figure 14. They show that in all cases p_b/p_∞ increases with increasing δ/h irrespective of airfoil thickness, trailing-edge thickness, Reynolds number, or boattail angle (within the limited range $-2.9^\circ \leq \beta \leq 5^\circ$ covered by the thickness group). A comparison of the measurements for each thickness ratio with the faired curve representing the average for all three thickness ratios shows a small but consistent effect of thickness ratio; the base pressure at a given value of $c/[h(Re)^{1/2}]$ is slightly lower for the thinner wings. This may be due to a tip-relieving effect associated with the finite span of the wings, since the span to base-height ratio varied from 15 (for wing 10-1.00) to 120 (for wing 5-0.25); or it may be due to some effect on the boundary layer which itself depends on airfoil-thickness ratio.

Base pressure measurements on each wing of the thickness group also were taken at $M_\infty = 1.5$ over the Reynolds number range between 0.2×10^6 and 1.7×10^6. As is evident from figure 15, the results for all wings having $t/c = 0.10$ or 0.075, and for some of the wings having $t/c = 0.05$, conform well with each other and with the trend described above for $M_\infty = 2.0$ and $M_\infty = 3.1$. For the two wings with the thinnest trailing edges (wings 5-0.25(R) and 5-0.50(R)), however, the base pressure is much lower at certain Reynolds numbers than would be expected on the basis of the average curve for the other wings. The base pressure data for wings 5-0.25(R) and 5-0.50(R) conform with the main body of data only at Reynolds numbers below about 0.5×10^6, corresponding to values of $c/[h(Re)^{1/2}]$ greater than 0.12 and 0.05, respectively. (See fig. 15(c).) It will be seen subsequently that these nonconforming base pressures do not persist to angles of attack above a few degrees, and that even at 0° the base pressure measurements on the thinnest wings can be made to

conform with the main body of data by employing a moderate boattail angle at the trailing edge. As a result, the nonconforming data do not appear at present to be of much practical importance. However, it also will be seen later that these data are accompanied by several unusual phenomena which are of considerable interest from the viewpoint of gas dynamics. Consequently, much of the discussion which follows is concerned with the few wings which exhibit the unexpectedly low base pressures.

A number of supplementary tests were conducted to investigate the nonconforming data in more detail. From these tests it was observed that although the base pressure measurements on wing 5-0.25(R) repeated reasonably well if the data were taken in the order of increasing Reynolds number, the measurements sometimes failed to repeat if the data were taken in the order of decreasing Reynolds number. This is illustrated in figure 16. The failure to repeat was observed only at intermediate Reynolds numbers. Measurements on other wings, and the measurements at higher Mach numbers (as well as all measurements with turbulent flow), could be repeated satisfactorily. The reason for the inability to repeat measurements taken under the special conditions just outlined is not known as yet. One explanation that immediately suggests itself is that transition from laminar to turbulent flow occurred in the boundary layer in this Reynolds number range. However, the china-clay pattern in figure 3(b) shows that the boundary layer was laminar to the trailing edge of wing 5-0.25(R) at a Reynolds number of 1.7×10^6. At the time this photograph was made, a similar pattern existed on the opposite surface of the wing. During this run, nonconforming base pressures were measured at all Reynolds numbers above about 0.5×10^6, just as was the case for the runs (fig. 16(a)) made without the china clay applied to the surfaces.

Supplementary tests also showed that the phenomenon responsible for the nonconforming (unexpectedly low) base pressures is not associated with a rounded ridge line. In fact, the ridge lines on wing 5-0.25, 5-0.50, and 7.5-0.25 were rounded during the course of the investigation in an attempt to alleviate this phenomenon. Measurements on these three wings showed that at all Reynolds numbers the effect of rounding the ridge line was of the same order as the differences in repeat runs on a given wing. In addition, it was found that the few nonconforming measurements were not associated with the center orifice position or with any one support, since the data for the inboard orifice position and three different supports (discussed in appendix A) showed the same unexpectedly low values of p_b/p_∞, and in some cases showed them over a wider Reynolds number range than indicated in figure 15(c). The phenomenon may be aggravated by support and model vibrations, however, since the sting support indicated low values of p_b/p_∞ even at the lower Reynolds numbers ($0.2 < Re \times 10^{-6} < 0.5$) where the measurements taken with the more rigid body supports always correlated with the main body of data.

Effect of boattail angle for laminar flow.- In figure 17 base pressure measurements on wings of both the boattail and thickness groups tested with smooth surfaces are plotted as a function of the boattail angle. For each curve the Reynolds number, support, orifice position, and trailing-edge thickness is constant. At a Mach number of 2.0 the curves in figure 17(a) indicate that in contrast to the results for turbulent flow (fig. 10), there are significant effects of boattail angle on base pressures when the boundary layer is laminar. The maximum variation between $\beta = 0^{\circ}$ and $\beta = 20^{\circ}$ would result in a base drag variation of approximately 20 percent. Similar results with smooth wings were found at this Mach number for trailing-edge thicknesses corresponding to $h/c = 0.0375$ and $h/c = 0.025$.

For a Mach number of 1.5, a trailing-edge thickness corresponding to $h/c = 0.0125$, and Reynolds numbers above about 0.5×10^{6}, much larger variations in p_b/p_{∞} with β were found, as illustrated in figure 17(b). In this case the maximum variation is such that the base drag for $\beta = 5^{\circ}$ is approximately one-half that for $\beta = 2.5^{\circ}$. It is of interest here to note that at a Mach number of 1.5 the effects of boattail angle are the largest for the same conditions under which the nonconforming values of base pressure are most prominent, namely, for wing 5-0.25(R), small boattail angles and Reynolds numbers above 0.5×10^{6}. Similarly, under conditions where the base pressure measurements on wing 5-0.25(R) correlated with the main body of data, namely, for Reynolds numbers below about 0.5×10^{6}, the corresponding effects of boattail angle were the smallest, as shown by the curve for $Re = 0.3 \times 10^{6}$ in figure 17(b). This suggests that the large effects of boattail angle may be interconnected with the mechanism responsible for the unexpectedly low base pressures. In view of this, the fairing of the curves in figure 17(b) between $\beta = 2.5^{\circ}$ and $\beta = 8^{\circ}$ is very uncertain. The true curve may be discontinuous in this range.

Effect of angle of attack for laminar flow.- Curves of base pressure versus angle of attack for wings of the thickness group tested with smooth surfaces at $M_{\infty} = 2.0$ are shown in figure 18. For most wings there is little effect of angle of attack within the range investigated (just as is the case for turbulent boundary-layer flow). For wings 10-0.25 and 5-0.25(R), there is a larger decrease in base pressure with increasing angle of attack than for the other wings. The same result was found for wing 7.5-0.25(R). The base pressure measurements in figure 18 were all taken at a constant Reynolds number of 1.0×10^{6}. Similar measurements for $M_{\infty} = 2.0$ at Reynolds numbers of 0.55×10^{6} and 1.4×10^{6} showed the same characteristics.

In comparison to the curves just described, the curves of base pressure versus angle of attack at $M_{\infty} = 1.5$ and $Re = 1.0 \times 10^{6}$ (fig. 19) are quite similar for wings having relatively thick trailing edges (see fig. 19(a)), but remarkably dissimilar for the two wings having the thinnest trailing edges. (See fig. 19(b).) In the latter case, the base pressure increases almost discontinuously when a certain angle of attack

is reached. Schlieren observations on a ground glass screen indicated that in certain cases the flow changed virtually instantaneously. Beyond the angle where p_b/p_∞ suddenly increased, the base pressure changed continuously, but not to a large extent. Base pressure measurements on wings with relatively thick trailing edges tested at $Re = 0.55 \times 10^6$ and $Re = 1.9 \times 10^6$ showed the same characteristics as those illustrated in figure 19(a) for $Re = 1.0 \times 10^6$. Similar measurements on wings with the thinnest trailing edges, however, showed that the curves of base pressure versus angle of attack depended to a great extent on the Reynolds number. This is illustrated in figure 20. Such measurements also revealed a hysteresis effect associated with changing angle of attack. Significant hysteresis effects were found only at $M_\infty = 1.5$ on the wings having the thinnest trailing edges, namely, wings 5-0.25(R), 7.5-0.25(R), and 5-0.50(R). Two types of hysteresis were observed. As illustrated in figure 21, these could be distinguished by whether or not the base pressure at $\alpha = 0^\circ$ was repeated after the angle of attack was increased to 5° and then brought back to 0°. Either type of hysteresis loop demonstrates that for special angles of attack two distinct flows are possible, both of which are stable to small variations in angle of attack.

In figure 22 two curves of p_b/p_∞ versus α are compared for wing 5-0.25(R). Each curve is for $Re = 1.3 \times 10^6$ and $M_\infty = 1.5$, but one represents the smooth wing and the other the same wing with a wire trip added. It is evident that the unexpectedly low values of p_b/p_∞ are not the same as the values for turbulent flow approaching the trailing edge. At $Re = 1.7 \times 10^6$, however, the values of p_b/p_∞ usually were reasonably close to the corresponding values for turbulent flow, in spite of the fact that china-clay photographs, such as shown in figure 3(b), indicated the boundary layer to be laminar at least up to the trailing edge. A possible explanation[1] of this and the unexpectedly low base pressures is that transition in these cases may have occurred in the separated boundary layer immediately downstream of the trailing edge.

Curves of base pressure versus angle of attack for several 5-percent-thick wings of the boattail group tested with smooth surfaces at $M_\infty = 1.5$ are shown in figure 23. These curves show that the discontinuous jump in base pressure (and presumably the attendant angle-of-attack hysteresis) does not occur for boattail angles between 5° and 20°. From this result it may be inferred that for wings with thin trailing edges tested at $M_\infty = 1.5$, the unusual effects of angle of attack are probably attributable to the same mechanism that is responsible for the large effects of boattail angle observed for values of β between 2.5° and 5°.

The effect of Mach number on base pressure at a constant Reynolds number is illustrated by the curves in figure 24. For wing 10-0.25, shown in part (a) of this figure, only a small effect of Mach number on

[1]This was suggested by H. L. Dryden.

base pressure is evident. For wing 5-0.25(R) (fig. 24(b)), which has a thinner trailing edge, a large effect is present indicating the unexpectedly low base pressures to be more prevalent at low supersonic Mach numbers than at $M_\infty = 1.5$ or higher. This same trend was found with wing 5-0.50(R) on which nonconforming base pressures ($p_b/p_\infty \approx 0.5$ at all $Re \geq 0.4 \times 10^6$) were measured at $M_\infty = 1.25$ for all angles of attack up to the maximum investigated ($\alpha = 5^\circ$). As is evident in figure 24(a), wing 10-0.25, although having the same trailing-edge thickness as wing 5-0.50(R), did not exhibit the unexpectedly low base pressures at $M_\infty = 1.25$. This may be due to the effect of boattail angle; on wing 10-0.25 the boattail angle is 5°, whereas on wing 5-0.50(R) it is 2.15°.

Several of the effects described previously are also evident on a plot of p_b/p_∞ versus the parameter $c/[h(Re)^{1/2}]$, as shown in figure 25. This figure illustrates the conditions under which the base pressure measurements on wing 5-0.25(R) correlated with the main body of measurements at $M_\infty = 1.5$. These conditions are: either (1) sufficiently low Reynolds numbers, or (2) proper boattail angle, or (3) moderate angle of attack. It appears that the nonconforming base pressures are characteristic of a combination of low supersonic Mach numbers, thin trailing edges, certain boattail angles, limited angle-of-attack range, and a certain Reynolds number range. The unexpectedly low values of p_b/p_∞ are not characteristic of any one of these individual items taken by itself.

For all wings described thus far the trailing edge was normal to the chord line. It was thought that the angle of inclination between the trailing edge and chord line might have an important effect on the nonconforming base pressures. A limited number of measurements were taken at $M_\infty = 1.5$ on one wing having $t/c = 0.048$ and $h/t = 0.19$ with the trailing edge progressively beveled so that it made an angle (φ) of 0°, 15°, 20°, 25°, 30°, 35°, 40°, and 45°, with the normal to the chord line. Only a moderate effect of the bevel angle φ on base pressure was noted in these measurements. In some cases the base pressure was lowered slightly, as illustrated by the curve for $\varphi = 15^\circ$ in figure 26, whereas in other cases it was increased, as illustrated by the curve for $\varphi = 25^\circ$. In no case did the measurements with a beveled trailing edge at the highest Reynolds numbers completely conform with the main body of data.

Schlieren Observations on Smooth Airfoils in a Two-Dimensional Channel

By employing the apparatus shown in figure 6, schlieren observations were made at $M_\infty = 1.5$ simultaneously with base pressure measurements on

two smooth airfoils having profiles as illustrated:

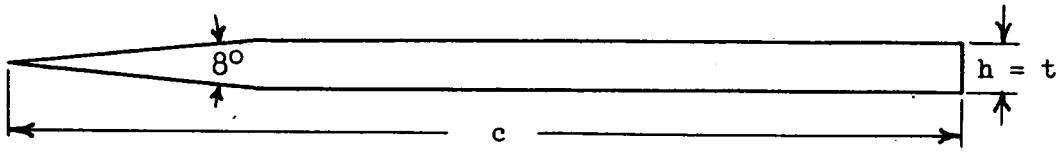

one with $t/c = h/c = 0.035$ and $c = 4.00$ inches, and the other with $t/c = h/c = 0.020$ and $c = 5.00$ inches. At certain Reynolds numbers the base pressure measurements on these airfoils at various angles of attack showed the same sudden jump in base pressure and the same attendant hysteresis effects as were described previously. Figure 27 shows flash schlieren photographs of the 3.5-percent-thick airfoil which illustrate the various types of wakes observed. An interesting feature of these photographs is the vortex street. (See fig. 27(a), for example.) Such vortices were observed only at angles of attack from zero up to the value at which the base pressure suddenly jumped. At this point the wake changed to a type involving disturbances but no pronounced vortex trail (for example, fig. 27(b)). For most of the schlieren photographs in which vortices were observed the spacing was less regular than shown in figure 27(a), indicating that the shedding was not entirely periodic. (See fig. 27(c).) Nevertheless, in these cases a predominant frequency usually could be detected on the oscilloscope. At the highest Reynolds numbers, the wake did not show pronounced vortices, but appeared to spread continuously downstream of the trailing shock wave. (See fig. 27(d).) Unfortunately, the location of transition is not known for the various types of wakes illustrated in this figure. The observation that the nonconforming base pressure measurements were more prevalent at the lower supersonic Mach numbers (1.25 and 1.5), taken together with the observation that the nonconforming measurements were associated with a vortex trail, suggests that the phenomenon actually may be a carry-over from the well-known phenomenon of vortex shedding at subsonic speeds which is pronounced for profiles of the type investigated here.

By using the oscilloscope and auxiliary apparatus described earlier, the predominant frequency of vortex shedding from the 2-percent-thick airfoil was found to vary only slightly with Reynolds number. The measured values were between 7×10^4 and 8×10^4 cycles per second. This frequency range corresponds to Strouhal numbers (fh/V_∞) between about 0.43 and 0.48. For comparison, the Strouhal number was estimated from several schlieren photographs by assuming that each vortex travelled downstream with the free-stream velocity. The Strouhal number estimated from figure 27(a), for example, is 0.57. This is in reasonable agreement with the measured values considering the fact that the vortices travel downstream at a velocity somewhat less than the free-stream velocity. It is interesting that for those cases where a regular vortex street was observed in the present tests at supersonic velocities, the

relative spacing between vortices (ratio of vertical spacing to horizontal spacing) was approximately the same as for subsonic velocities, but the Strouhal number based on trailing-edge thickness was about twice as great.

Comparison of Results With Theoretical Estimates and With Similar Measurements on Bodies of Revolution

Although no theory has yet been developed which considers all known variables that affect base pressure, Cope (reference 9) and Kurzweg (reference 10) have advanced approximate analyses which predict a variation of base pressure with the boundary-layer thickness. Cope's equations were given explicitly only for axially symmetric flow, but the corresponding equations for two-dimensional flow are easily derived. A comparison of the calculated values with the present experiments at a Mach number of 2.0 showed poor agreement. In fact, for both laminar and turbulent flow, Cope's analysis predicts a thrust force on the base for most of the range of values of δ/h covered in the present tests. Kurzweg's equations, which give the same base pressure for airfoils as for bodies of revolution, also do not yield satisfactory results when applied to airfoils. The calculated values at a Mach number of 2.0 represent base drags of approximately one-half of the experimental values for turbulent flow, and about two to three times the corresponding values for laminar flow.

By way of comparison with similar measurements on bodies of revolution, it may be noted that the effect of Reynolds number on base pressure, as indicated by the present tests, is much the same for airfoils as has already been found for bodies: It is small for turbulent flow, but large for laminar flow (particularly at low Reynolds numbers). On the other hand, the effect of boattail angle on base pressure for turbulent flow at low supersonic Mach numbers is remarkably different for airfoils than for bodies: It is small for airfoils, but large for bodies of revolution. With turbulent boundary-layer flow the base pressure is much lower for airfoils than for bodies at low supersonic Mach numbers, but appears to be nearly the same for airfoils and bodies at high supersonic Mach numbers.

CONCLUDING REMARKS

From an engineering viewpoint the principal practical results of the present investigation can be presented in two plots giving the various mean curves of base pressure versus $c/[h(Re)^{1/5}]$ and $c/[h(Re)^{1/2}]$. For convenience such curves are shown together in figure 28. The curves

for turbulent flow (fig. 28(a)) represent average values for the two orifice positions tested. The curves for laminar flow are the same as those shown in figures 14 and 15.

In general, the effects of angle of attack, boattail angle, and profile shape on base pressure appear to be closely tied together in the sense that when one effect is small the other two are small, and when one effect is large the other two also are large. Thus, with turbulent flow all effects were small. With laminar flow all three effects on base pressure were moderate for most cases, but all three were large for the special conditions associated with the nonconforming data.

A large part of the present investigation has been concerned with the few wings and special conditions under which the measured base pressures did not conform with the main body of data for laminar flow. Such special conditions, together with the attendant vortex trail and sudden jump in base pressure, appear to be of interest primarily as gas-dynamic phenomena. It is noted that the attention paid to these phenomena is out of proportion to their present relative practical value inasmuch as the results showed, for example, that with turbulent boundary-layer flow no such phenomena were present, and that all data for turbulent flow correlated satisfactorily. Also, with laminar boundary-layer flow such phenomena were not observed except when all the following conditions were satisfied simultaneously: low supersonic Mach number, thin trailing edge, certain Reynolds number range, small boattail angle, and small angle of attack.

Ames Aeronautical Laboratory
National Advisory Committee for Aeronautics
Moffett Field, Calif., Oct. 29, 1951

APPENDIX A

INVESTIGATION OF THE EFFECTS OF THE VARIOUS SUPPORTS ON BASE PRESSURE

As discussed earlier, strength considerations required that several different supports be used to mount the wings in the wind tunnels. This enabled considerable data to be obtained on the effects of support interference on base pressure.

Measurements using boundary-layer trips.- In figure 29 base pressure data are presented which were obtained at Mach numbers of 1.5 and 2.0 with the thickness group of wings mounted on various supports in the No. 1 wind tunnel. With the sting support, a 3/4-inch band of lampblack was employed as a boundary-layer trip to insure turbulent flow. With the short body No. 1 and long body No. 1 supports, a 0.005-inch wire was used as a boundary-layer trip. All experimental points shown in figure 29 were obtained with the base pressure orifice in the inboard position. Shown for comparison is the mean curve for the data obtained with the systematic group of wings tested on the short body No. 2 with wire trips and the orifice at the center position. It can be seen that the base pressure was affected only to a small extent by the changes in the shape of the support body and the orifice location. Similar results were observed at Mach numbers of 1.5 and 3.1.

Measurements on smooth wing surfaces.- The effect of body shape was also investigated with laminar boundary layers at Mach numbers of 1.5, 2.0, and 3.1. From the photographs of the china-clay transition patterns (see fig. 3) it can be seen that a turbulent region existed on the surfaces of the wings adjacent to the body-type supports. Presumably this was caused by transverse contamination originating at the wing-body juncture. Since the inboard orifice position was on the boundary of this region when the body-type supports were used, one might expect that the base pressure as measured at this orifice position would be considerably different for a wing mounted on the sting from that on the same wing mounted on a body-type support. However, the data for several representative wings shown in figure 30 indicate that this usually was not the case. The only apparent variation of base pressure with support shape occurred on wing 5-0.25. It was found that with the sting support at a Mach number of 1.5, unexpectedly low base pressures were measured at all Reynolds numbers, instead of just above $Re = 0.5 \times 10^6$ as was the case for other supports.

At a Mach number of 3.1, the china-clay technique indicated that the shock wave originating at the nose of the body-type supports interacted with the boundary layer on the wing to produce a disturbance which was visible in the china-clay pattern. (See fig. 3(d).) Since this disturbance occurred at the spanwise station of the center orifice position when

the short body was used, the data presented for smooth wings at this Mach number were obtained with the long body. The china-clay photographs for the long body (see fig. 3(c)) indicate that the center orifice position is free of such disturbances. Although the base pressure measurements at $M_\infty = 3.1$ with the long and short bodies did not differ appreciably when a trip was used, the corresponding measurements did differ significantly when certain wings were tested smooth. With the shorter body, the measured base pressure at the center orifice on wings with the thinnest trailing edges was lower than with the longer body, and hence closer to the corresponding base pressure for turbulent flow.

The support and orifice position employed in obtaining the data presented in each figure of this report is listed in the table which follows.[2]

Support \ Orifice	Inboard	Center	Survey tube
Sting	Figs.10(b),17(a)	- - -	- - -
Short No. 1	- - -	- - -	Figs. 7, 12
Short No. 2	- - -	Figs.8(a),8(b),9, 10(a),11,14,15,16, 17(b),18,19,20,21, 22,23,24,25,26	- - -
Long No. 2	- - -	Figs. 8(c), 13	- - -

[2]This table does not include figures 29, 30, and 31, which compare the data for various supports and orifice positions.

APPENDIX B

INVESTIGATION OF VARIOUS BOUNDARY-LAYER TRIPS

At the highest tunnel pressure in the No. 1 wind tunnel, the Reynolds number based on the 3-inch chord of the wings was approximately 1.7 million. At this and lower Reynolds numbers, laminar flow would be expected over the entire surface of the wings. This expectation was verified by the china-clay technique previously described. In order to obtain data in the No. 1 wind tunnel with turbulent boundary layers approaching the trailing edge of the wings, it was necessary to induce transition by some artificial means. A 3/32-inch band of salt crystals, bands of lampblack grains of various band widths, and a 0.005-inch-diameter wire were investigated to determine their effectiveness as boundary-layer trips when cemented to the surface of the wings near the leading edge. Base pressure measurements were made with each of these devices on wing 10-0.25 at a Mach number of 2.0. The results are shown in figure 31. Also shown in this figure are data for the same wing without a boundary-layer trip obtained in both the No. 1 and the No. 2 wind tunnels. From observations with the china-clay technique, it was concluded that the lower base pressures which were essentially independent of Reynolds number are associated with turbulent flow. Therefore, transition appears to have been complete above a Reynolds number of 1.4 million for all the trips, and above 1.0 million for some of the trips. At Reynolds numbers above 1.4×10^6, the base pressure for all practical purposes was independent of the trip employed and agreed very well with the data obtained at higher Reynolds numbers without a trip in the No. 2 wind tunnel. It can be seen that the variation of base pressure with Reynolds number is not continuous for the smooth wing when the data from both tunnels are considered. The boundary layer is apparently laminar at Reynolds numbers near 1.9 million in the No. 1 wind tunnel, but turbulent at the same Reynolds number in the No. 2 wind tunnel. This situation is probably due to the known fact that the turbulence level is higher in the No. 2 wind tunnel. However, for most of the wings when tested smooth in the No. 2 tunnel, the curve of base pressure versus Reynolds number was not flat, indicating that transition usually occurred at some Reynolds number above the minimum in the No. 2 wind tunnel.

It can be seen that the 3/4-inch band of lampblack and the 0.005-inch wire caused transition to occur at approximately the same Reynolds number. Both of these trips were employed to obtain data representative of turbulent flow in the No. 1 wind tunnel. In general, the band of lampblack was used with the sting support and the wire was used with the body-type supports. This division was dictated by the convenience with which the two trips could be installed in conjunction with the supports.

At a Mach number of 3.1 the base pressure on most wings of the thickness group was measured separately with a 0.010-inch-diameter wire trip and a 0.005-inch-diameter wire trip. The larger wire was investigated because china-clay photographs indicated that at this Mach number the smaller wire effected transition only a short distance upstream of the trailing edge (instead of shortly downstream of the wire as was the case for the other Mach numbers). The observed differences in base pressure, however, were small. This may be seen by comparing the data at zero angle of attack in figure 11(b), which were taken with a 0.005-inch-diameter wire, with the corresponding data and faired curve in figure 8(c), which were taken with a 0.010-inch-diameter wire.

REFERENCES

1. Busemann, A., and Walchner, O.: Airfoil Characteristics at Supersonic Speeds. RTP Trans. No. 1786, British Ministry of Aircraft Production. (From Forschung auf dem Gebiete des Ingenieurwesens, March-April 1933, vol. 4, pp. 87-92)

2. Valensi, J., and Pruden, F. W.: Some Observations on Sharp Nosed Profiles at Supersonic Speed. R.&M. No. 2482, British A.R.C., 1947.

3. Chapman, Dean R.: An Analysis of Base Pressure at Supersonic Velocities and Comparison With Experiment. NACA TN 2137, 1950.

4. Chapman, Dean R.: Airfoil Profiles Having Minimum Pressure Drag at Supersonic Velocities - General Analysis With Application to Linearized Supersonic Flow. NACA TN 2264, 1951.

5. Richards, E. J., and Burstall, F. H.: The "China-Clay" Method of Indicating Transition. R.&M. No. 2126, British A.R.C., 1945.

6. Gazley, Carl, Jr.: The Use of the China-Clay Lacquer Technique for Detecting Boundary-Layer Transition. Rept. No. 49/A0536, General Electric Co., March 1950.

7. Lawrence, Leslie F., Schmidt, Stanley F., and Looschen, Floyd W.: A Self-Synchronizing Stroboscopic Schlieren System for the Study of Unsteady Air Flows. NACA TN 2509, 1951.

8. Allen, H. Julian, and Perkins, Edward W.: A Study of the Effects of Viscosity on the Flow Over Slender Inclined Bodies of Revolution. NACA Rep. 1048, 1951.

9. Cope, W. F.: The Effect of Reynolds Number on the Base Pressure of Projectiles. British NPL Eng. Div. Rept. 63/44, Jan. 1945.

10. Kurzweg, H. H.: Interrelationship Between Boundary Layer and Base Pressure. Jour. Aero. Sci., vol. 18, no. 11, Nov. 1951.

Table I

Dimensions of the Wings Employed In the Investigation

A. The Thickness Group

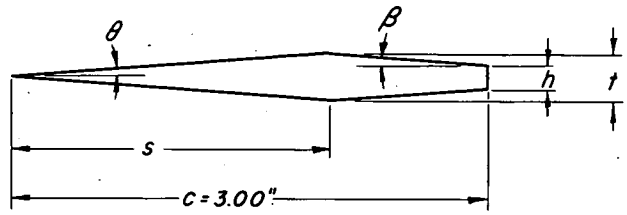

Wing 10-0.50

t/c (%) h/t

$\theta = \beta$ for all wings in this group

Wing Designation	Position of Max. Thickness s/c	Boattail Angle β	Airfoil Section
10-0.25	0.572	5.00°	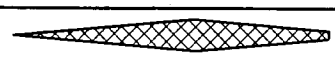
10-0.50	.667	4.28°	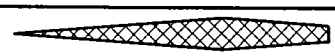
10-0.75	.800	3.58°	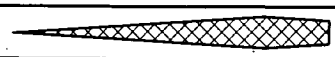
10-1.00	1.000	-2.87°	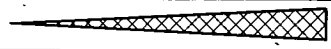
*7.5-0.25	.572	3.75°	
7.5-0.50	.667	3.22°	
7.5-0.75	.800	2.68°	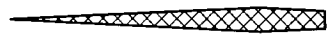
7.5-1.00	1.000	-2.15°	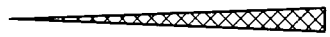
* 5-0.25	.572	2.50°	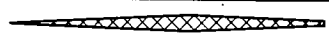
* 5-0.50	.667	2.15°	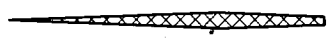
5-0.75	.800	1.78°	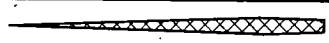
5-1.00	1.000	-1.43°	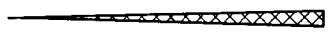

* The ridge lines on these wings were rounded during the course of the investigation

Table I.- Concluded

B. The boattail group.

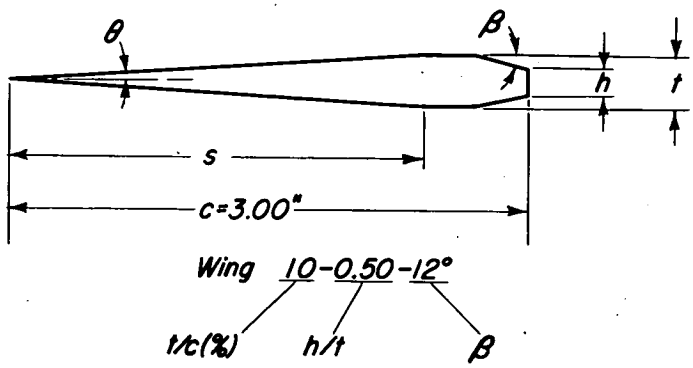

Wing	h/c	s/c	θ	Airfoil Section
10-0.50-20°	0.0500	0.800	3.58°	
10-0.50-16°	.0500	.800	3.58°	
10-0.50-12°	.0500	.800	3.58°	
10-0.50-7.1°	.0500	.800	3.58°	
5-1.00-0°	.0500	.800	1.78°	
5-0.50-16°	.0250	.800	1.78°	
5-0.50-12°	.0250	.800	1.78°	
5-0.50-8°	.0250	.800	1.78°	
5-0.50-3.6°	.0250	.800	1.78°	
*5-0.25-20°	.0125	.572	2.50°	
5-0.25-14°	.0125	.572	2.50°	
5-0.25-11°	.0125	.572	2.50°	
5-0.25-8°	.0125	.572	2.50°	
5-0.25-5°	.0125	.572	2.50°	

* The 5-0.25-β group was tested with rounded ridge lines.

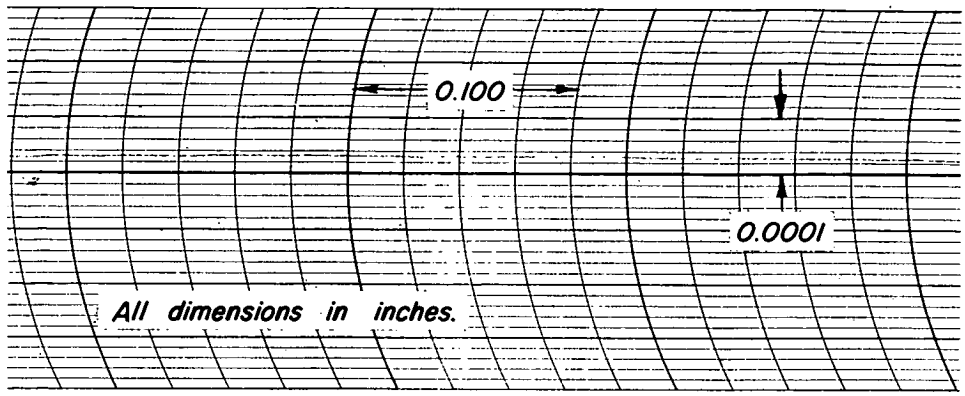

(a) Surface with typical roughness.

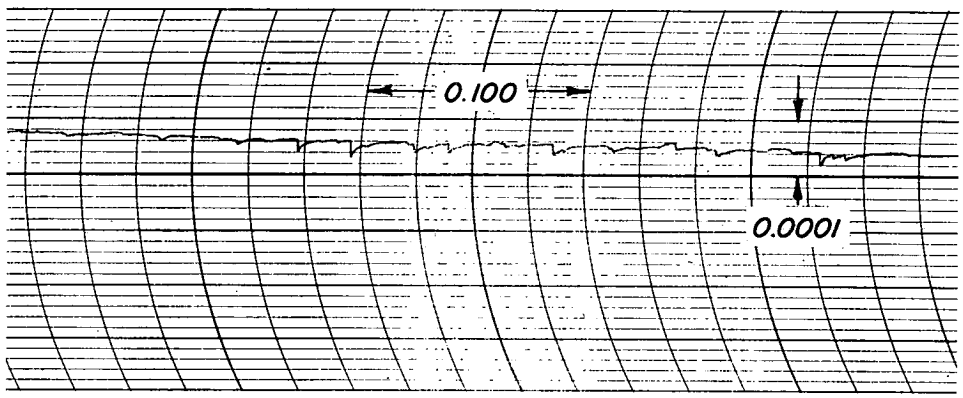

(b) Surface with maximum roughness.

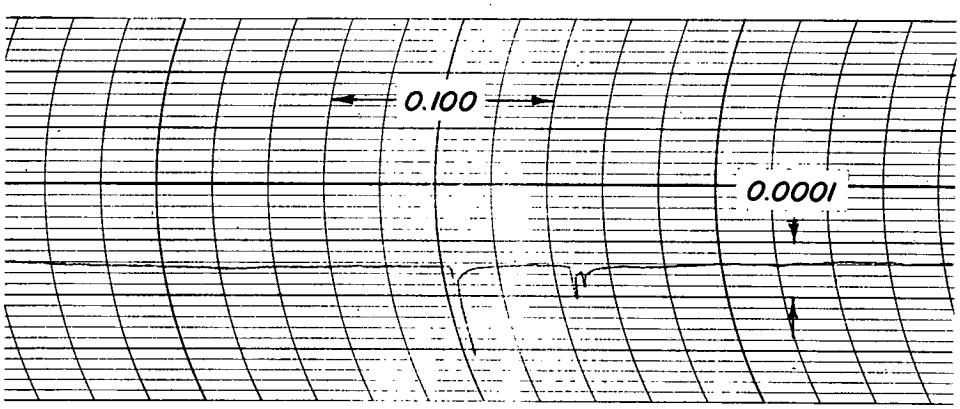

(c) Surface with scratch.

Figure 1.- Typical records illustrating the surface roughness of the wings; radius of tracing stylus = 0.0005 inch.

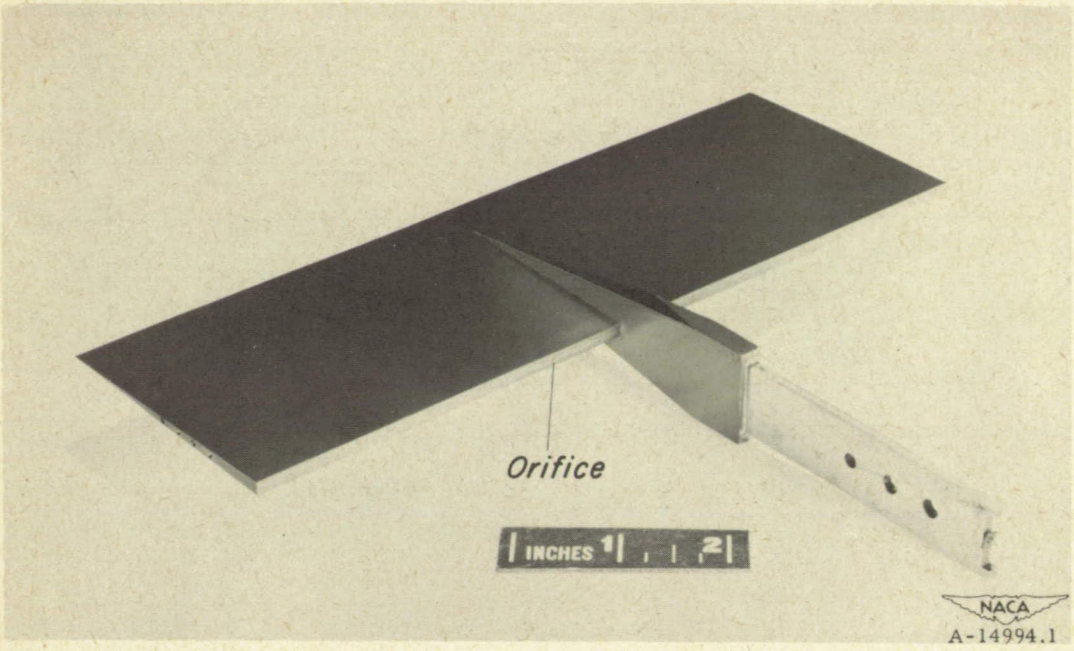

(a) Sting support.
(Shown with wing 5–1.00)

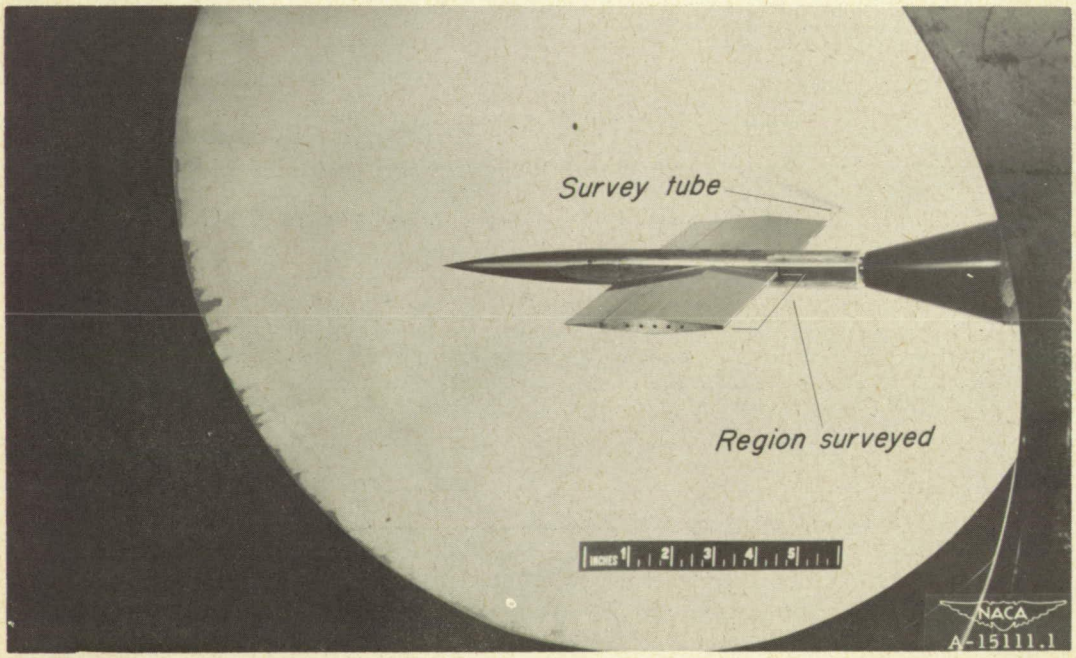

(b) Short body No. 1.
(Shown with the transverse survey probe installed on wing 10–0.25)

Figure 2.– Various supports used in the investigation.

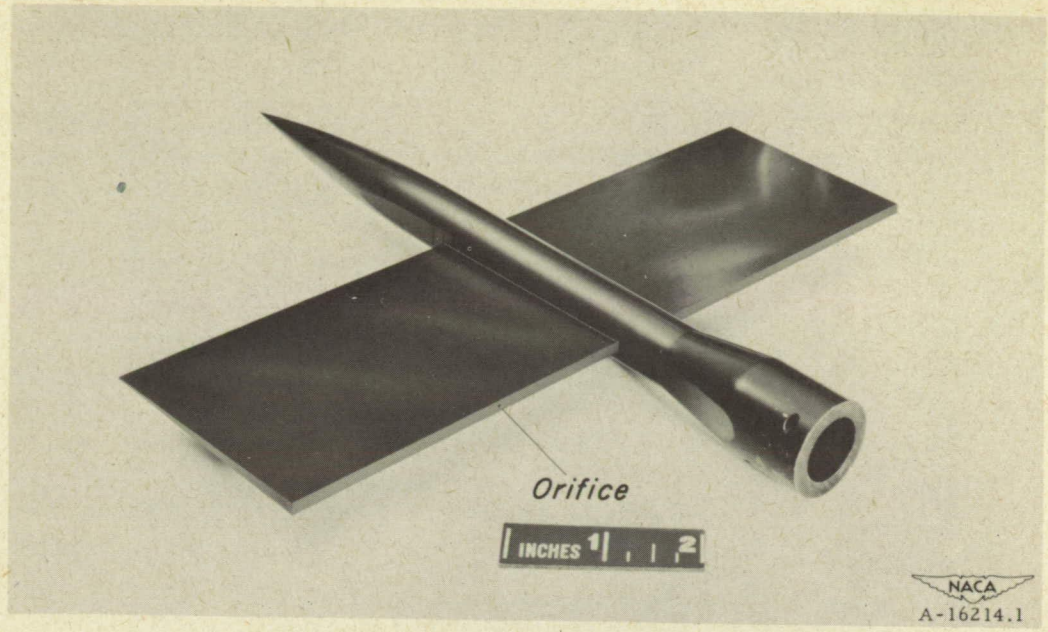

(c) Short body No. 2.
(Shown with wing 5-1.00.)

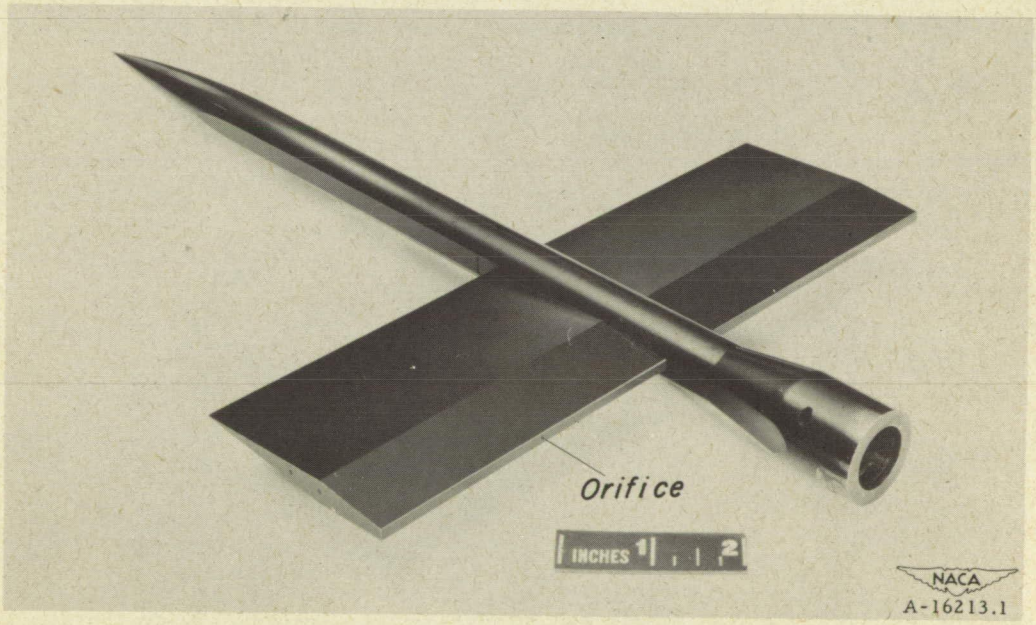

(d) Long body No. 2.
(Shown with wing 10-0.50.)

Figure 2.- Concluded.

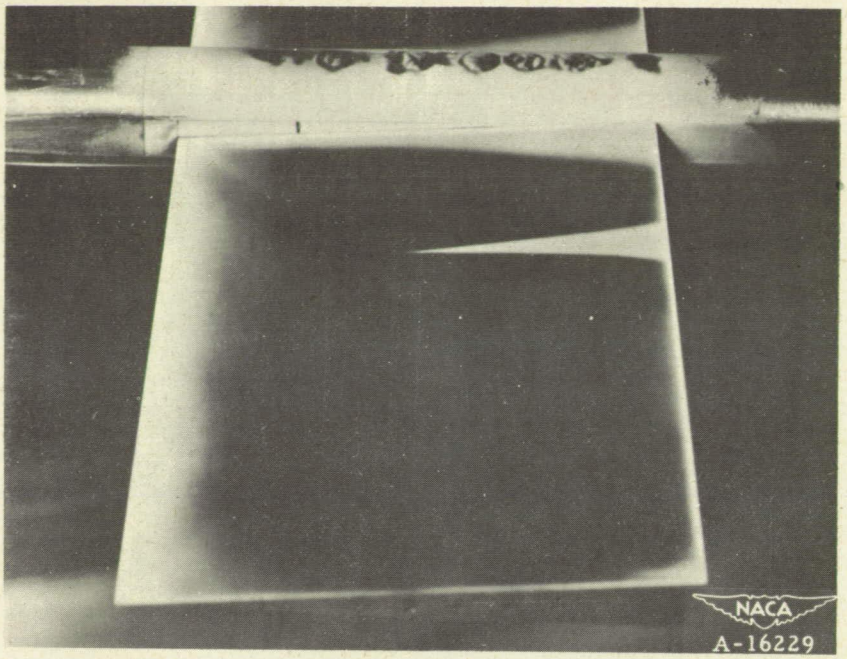

(a) Wing 10-1.00, short body No. 2;
$M_\infty = 1.5$, $Re = 1.7 \times 10^6$

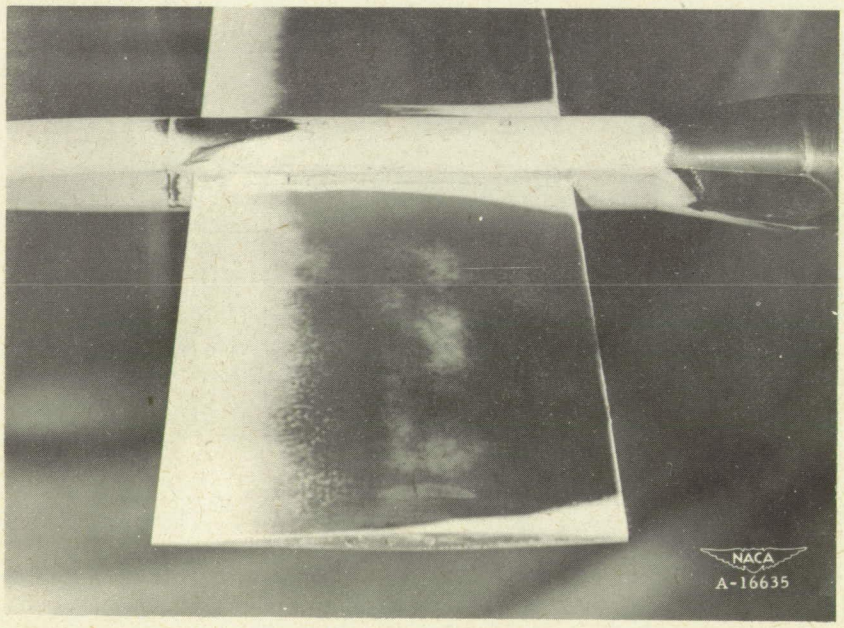

(b) Wing 5-0.25(R), short body No. 2;
$M_\infty = 1.5$, $Re = 1.7 \times 10^6$

Figure 3.- Typical china-clay photographs of wings with smooth surfaces.

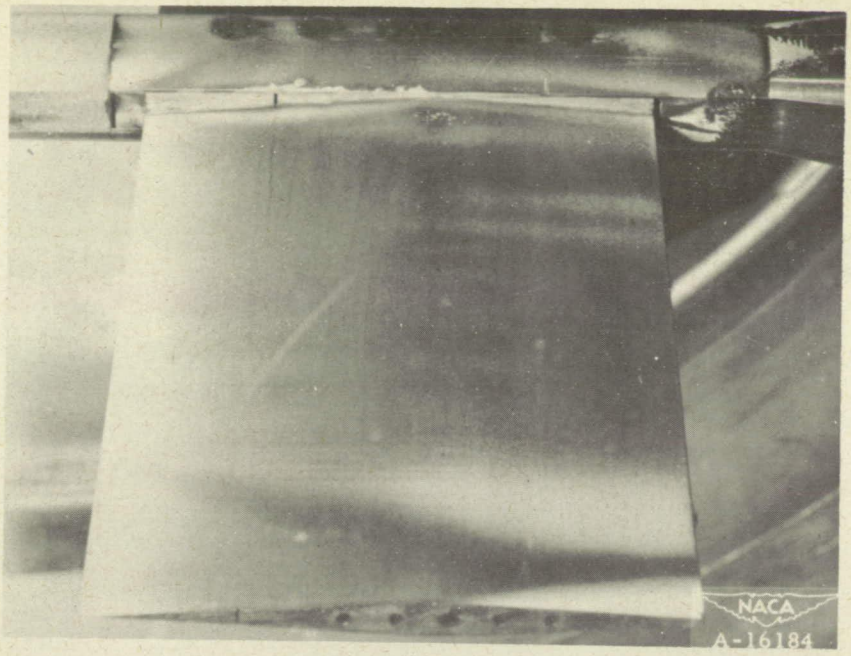

(c) Wing 7.5-0.25(R), long body No. 2;
$M_\infty = 3.1$, $Re = 2.2 \times 10^6$

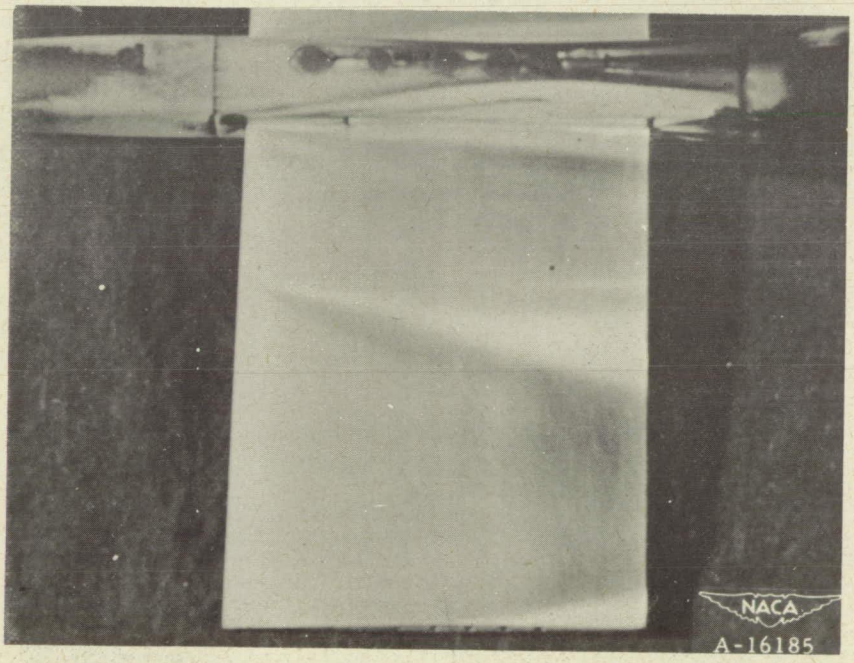

(d) Wing 5-0.25(R), short body No. 2;
$M_\infty = 3.1$, $Re = 2.2 \times 10^6$

Figure 3.- Concluded.

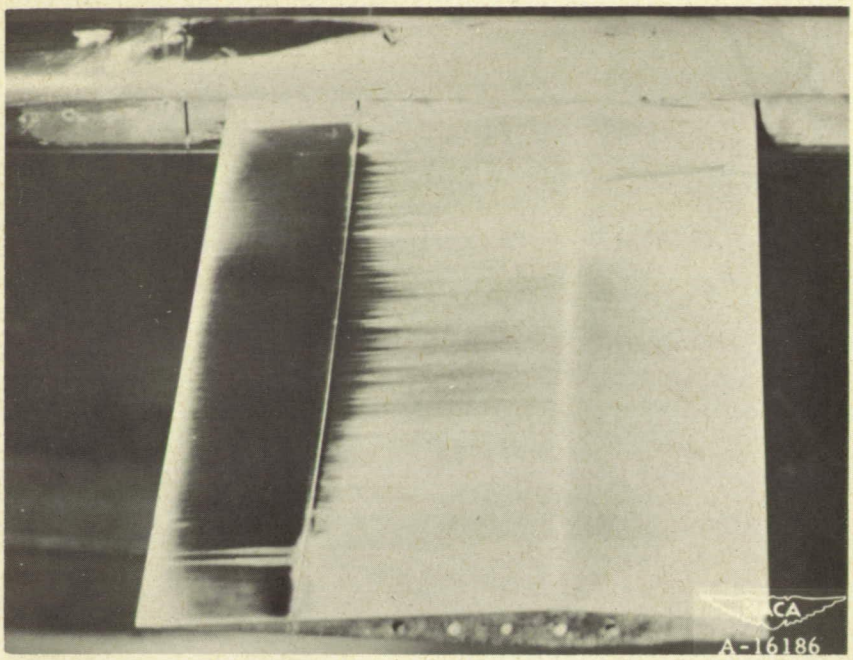

(a) Wing 7.5-0.50, short body No. 2;
$M_\infty = 1.5$, $Re = 1.1 \times 10^6$

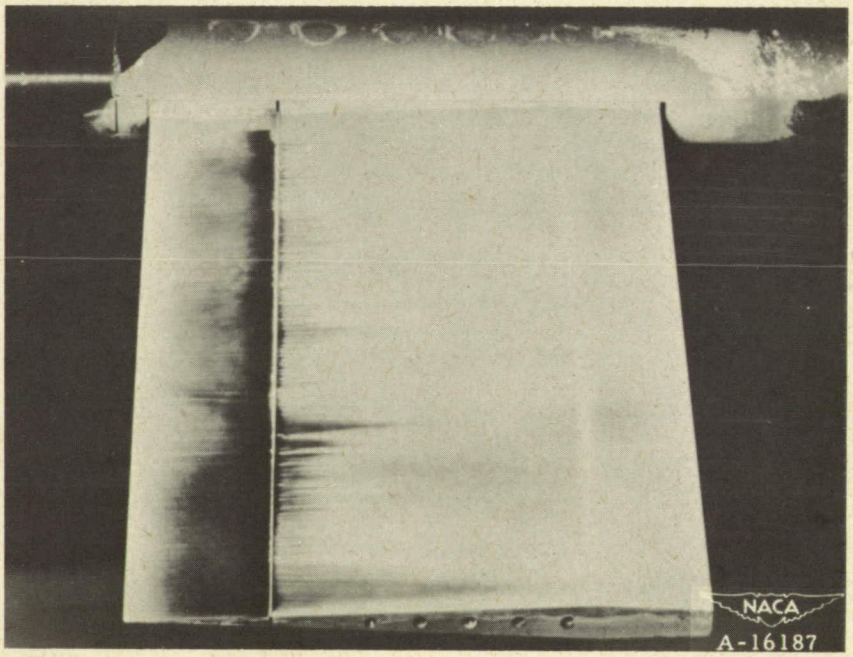

(b) Wing 7.5-0.75, short body No. 2;
$M_\infty = 2.0$, $Re = 1.1 \times 10^6$

Figure 4.- Typical china-clay photographs of wings with wire trips.

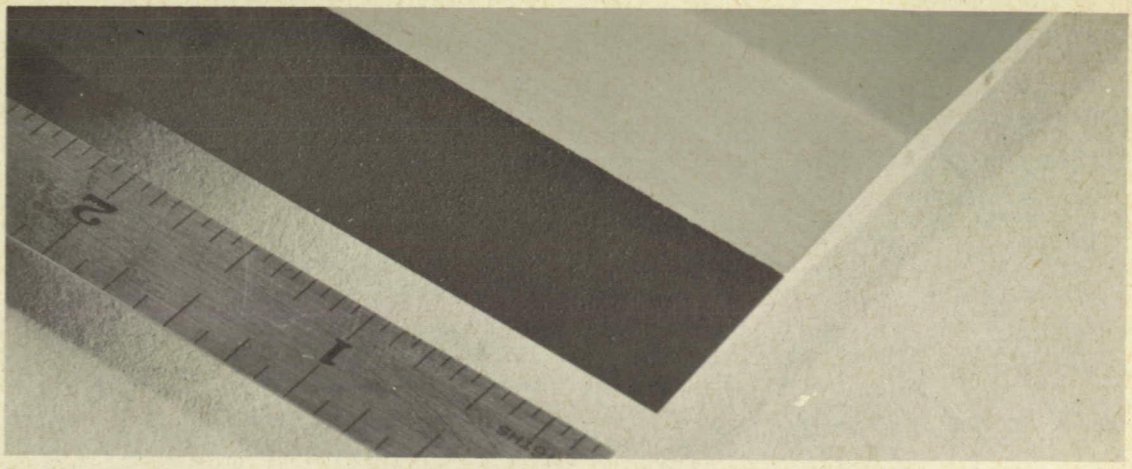

(a) Lampblack.

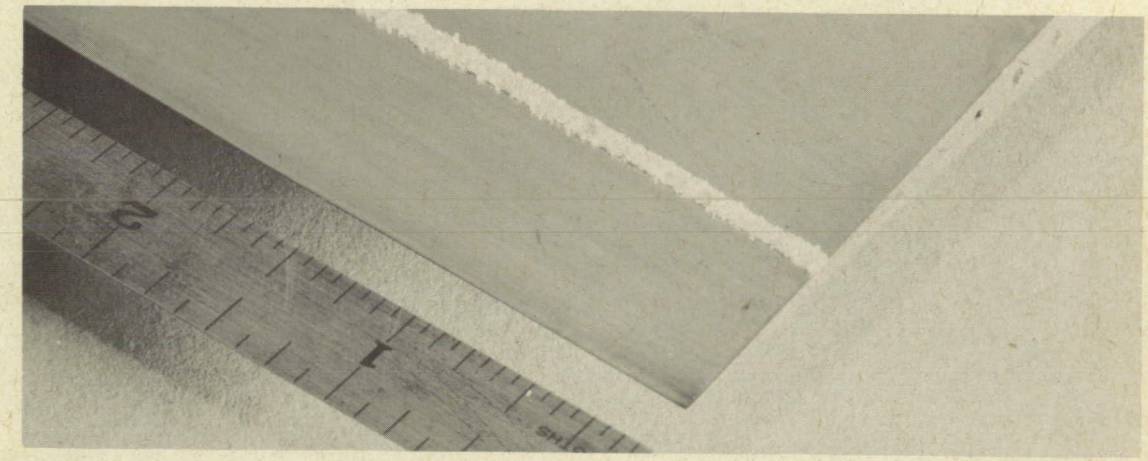

(b) Salt band.

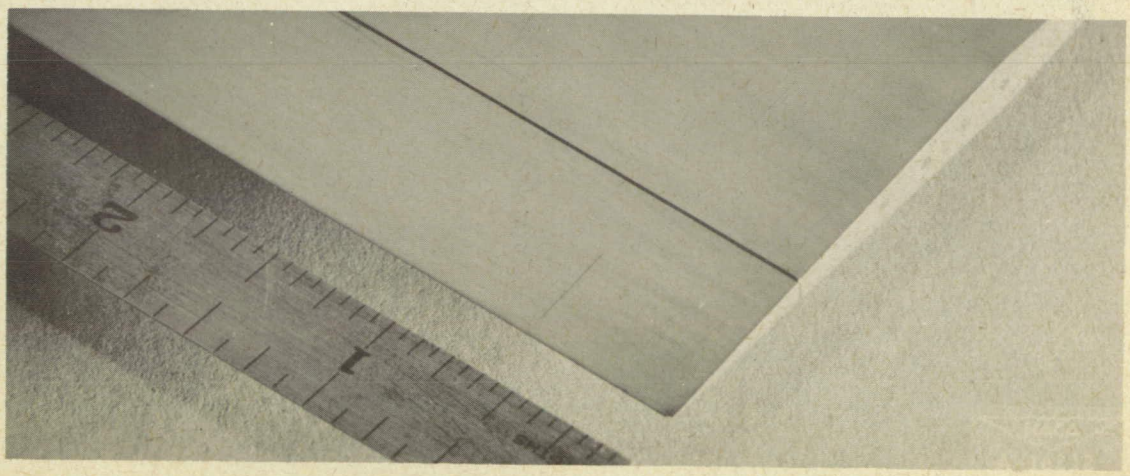

(c) 0.005-inch wire.

Figure 5.- Various boundary-layer trips investigated.

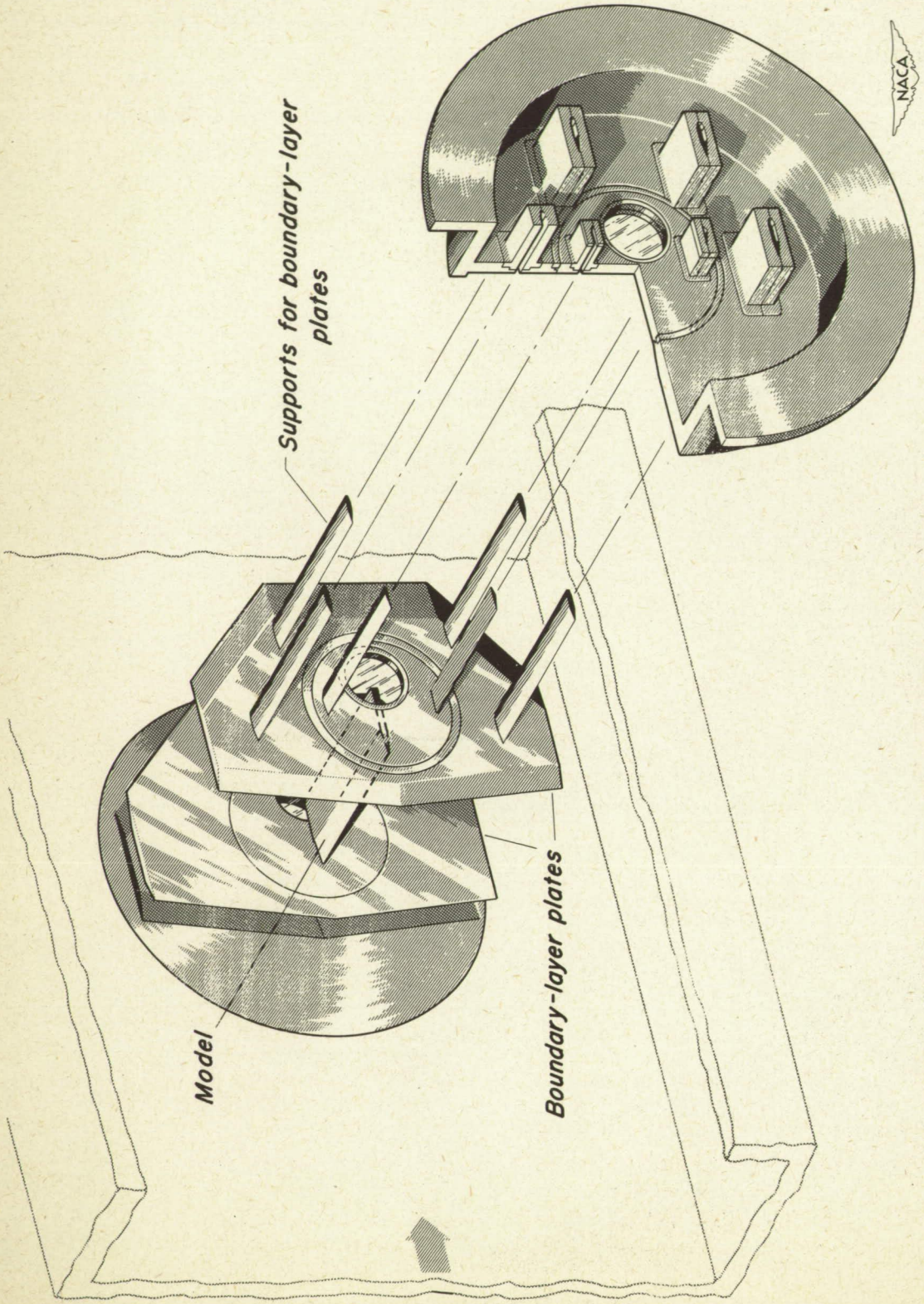

Figure 6.- The two-dimensional channel employed for schlieren observations.

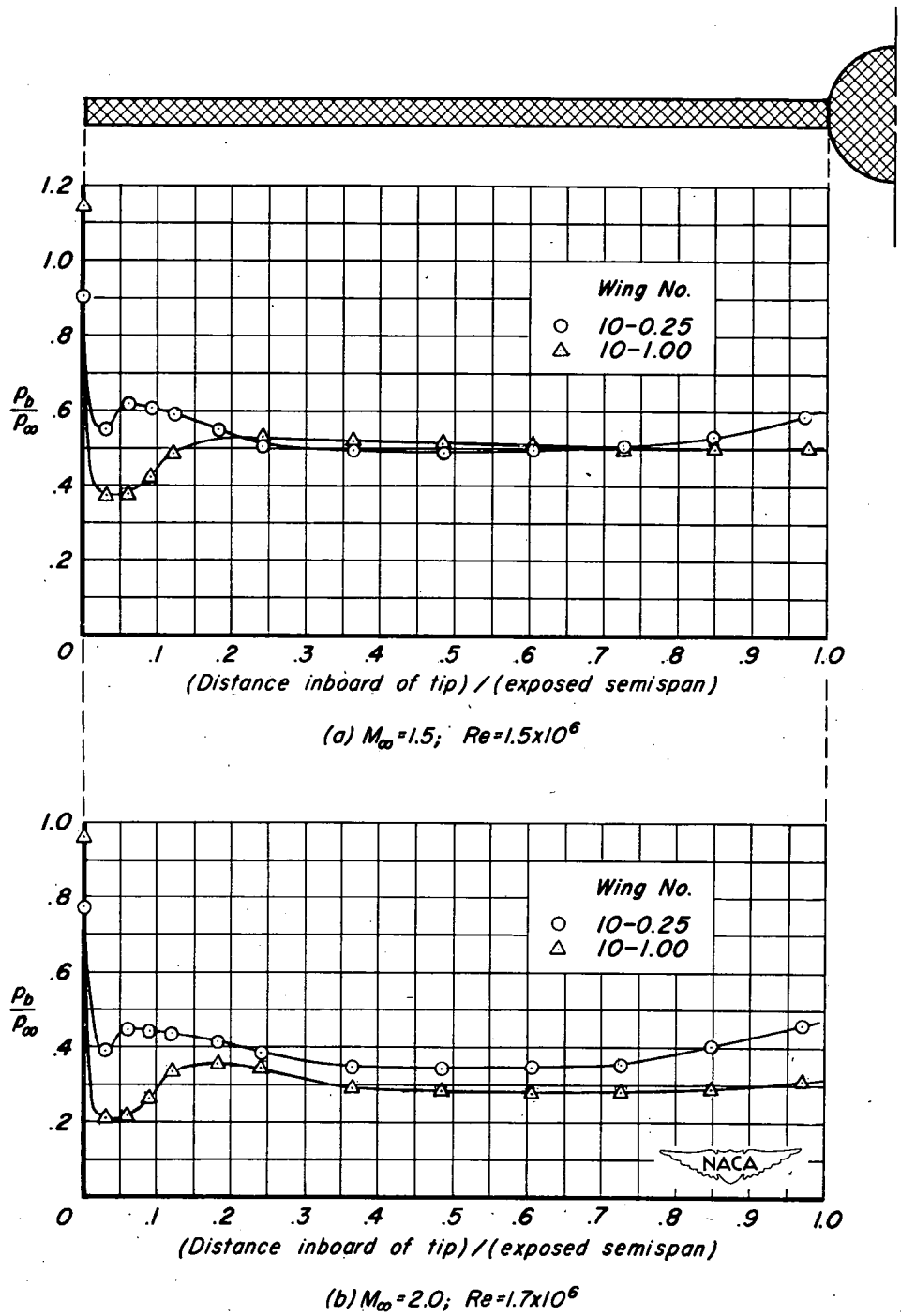

Figure 7.– Spanwise variation of base pressure for turbulent boundary-layer flow.

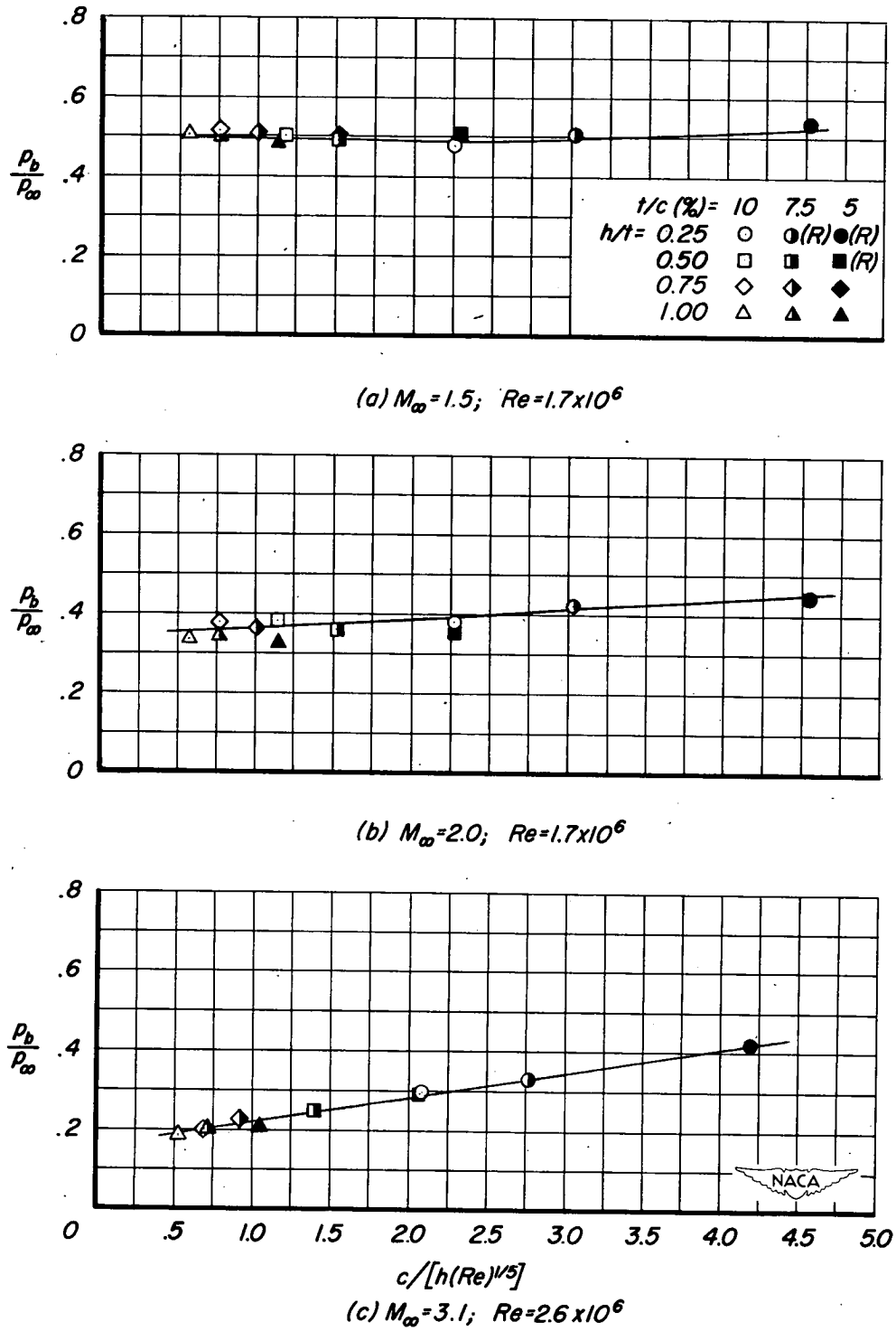

Figure 8.—Base pressure measurements on the thickness group of wings with turbulent flow.

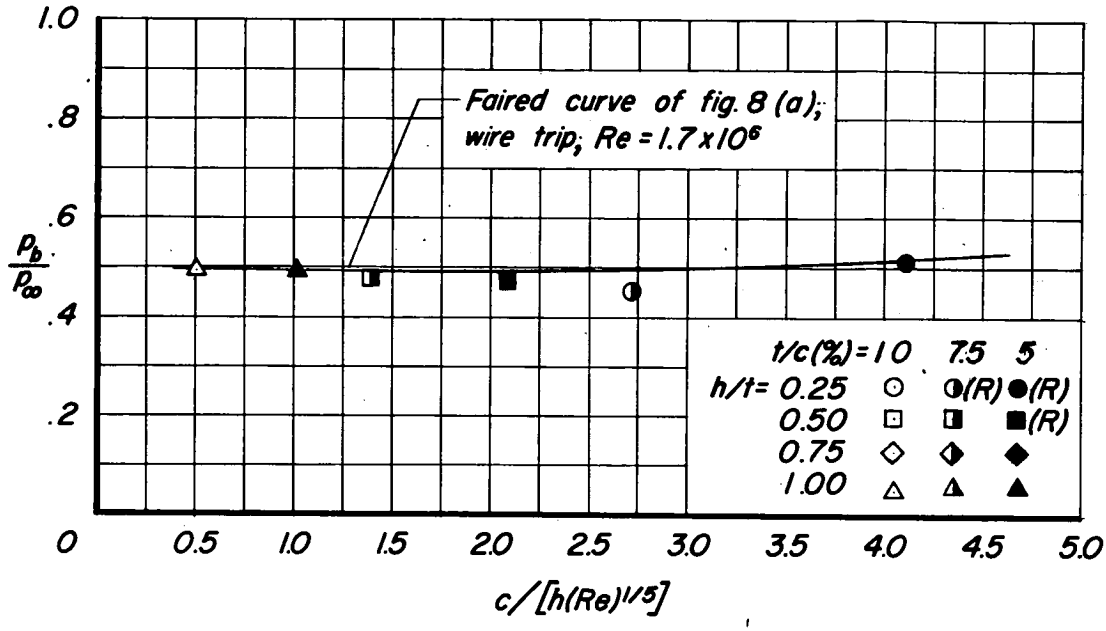

(a) $M_\infty = 1.5$; $Re = 3.0 \times 10^6$

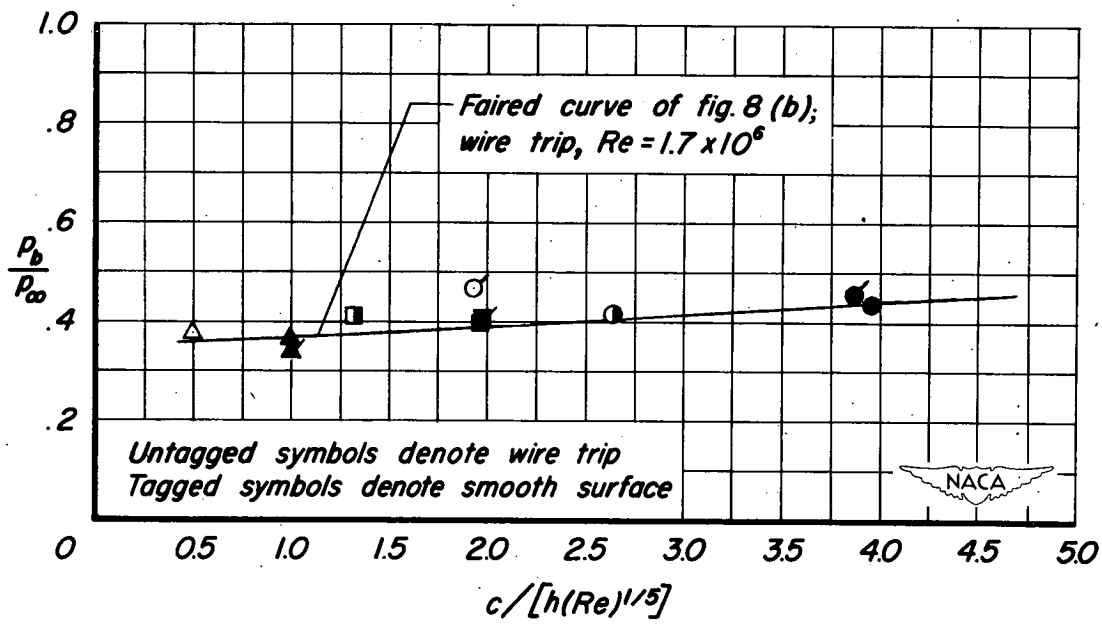

(b) $M_\infty = 2.0$; $Re = 3.5 \times 10^6$

Figure 9.—Comparison of base pressure measurements on the thickness group of wings with turbulent flow at different Reynolds numbers.

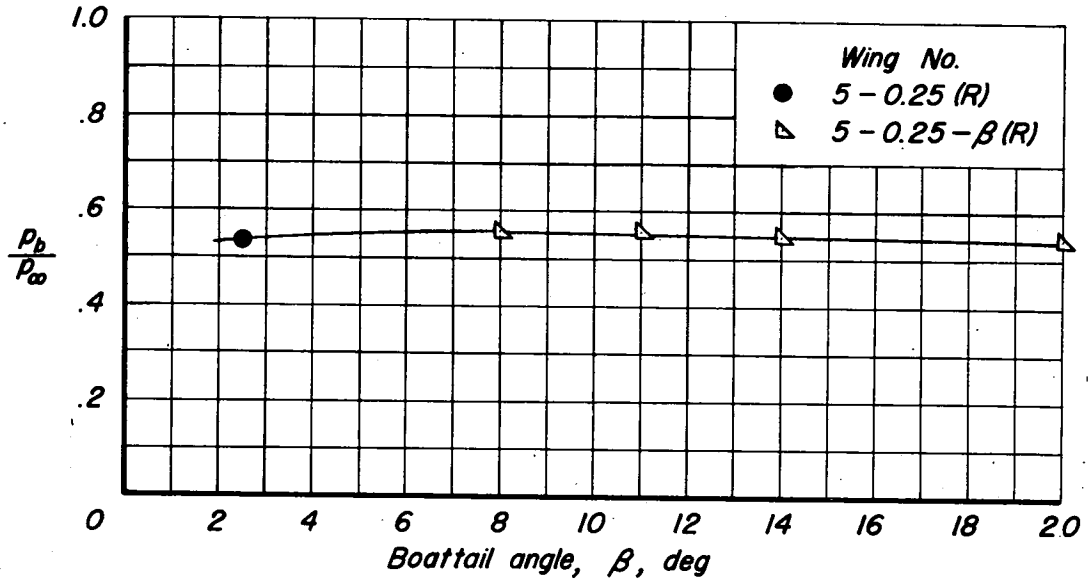

(a) $M_\infty = 1.5$; $Re = 1.7 \times 10^6$; $h/c = 0.0125$

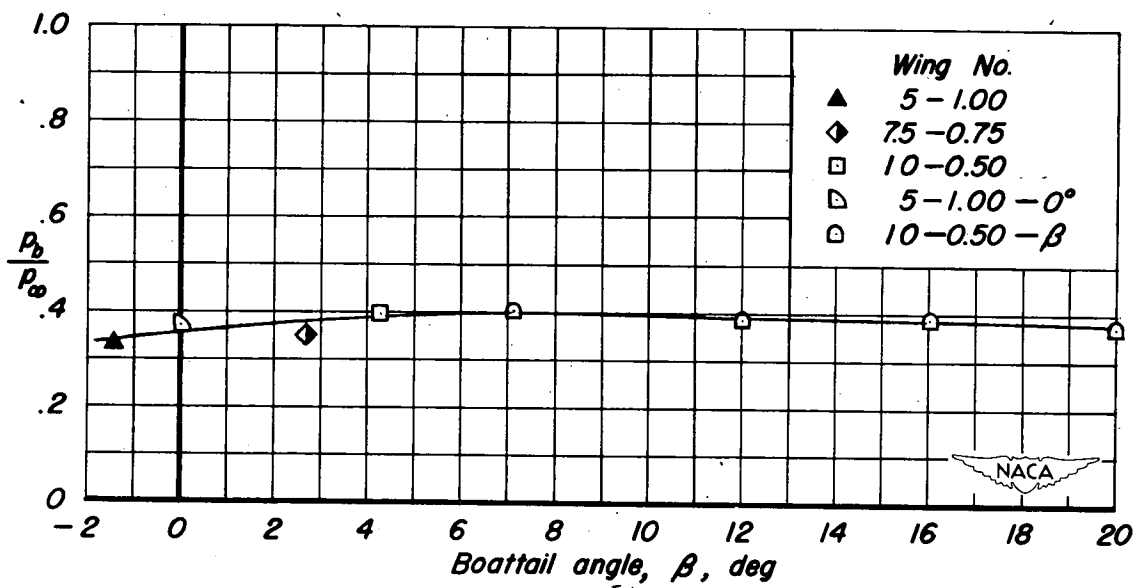

(b) $M_\infty = 2.0$; $Re = 1.7 \times 10^6$; $h/c = 0.05$

Figure 10.—Effect of boattail angle on base pressure with turbulent flow.

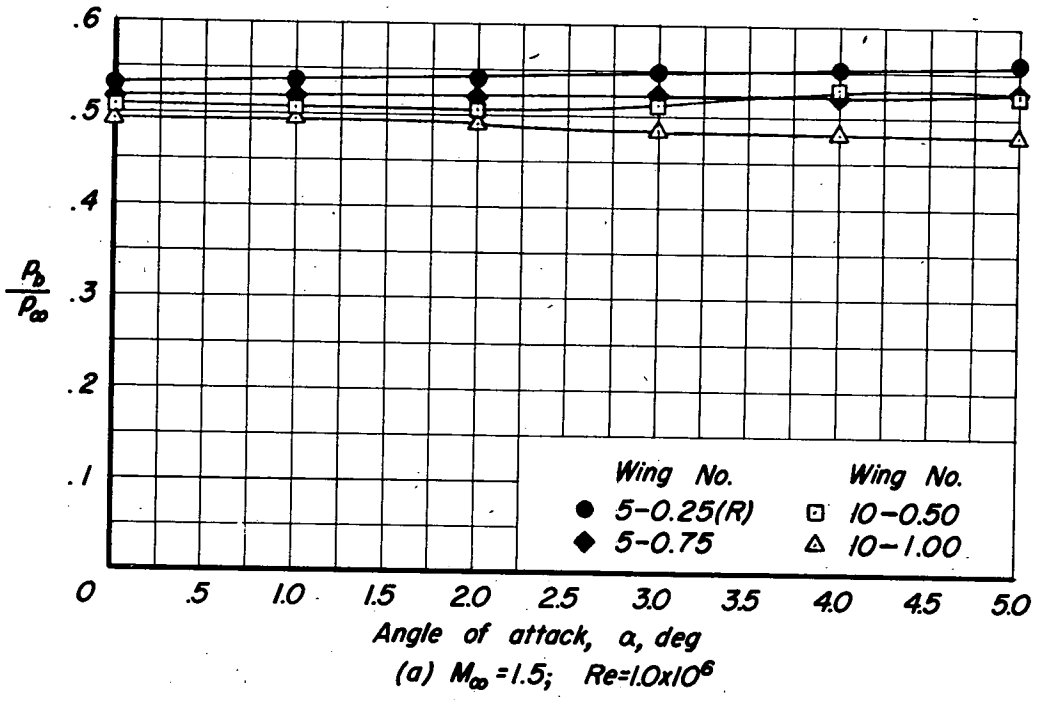

(a) $M_\infty = 1.5$; $Re = 1.0 \times 10^6$

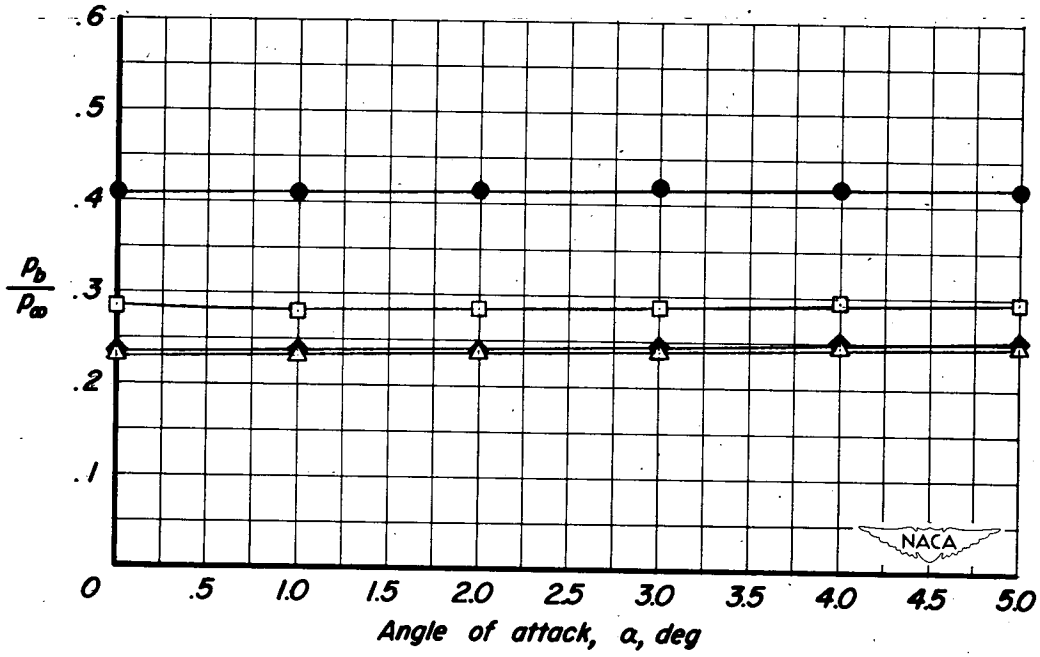

(b) $M_\infty = 3.1$; $Re = 2.3 \times 10^6$

Figure 11.– Effect of angle of attack on base pressure for turbulent flow on the thickness group of wings.

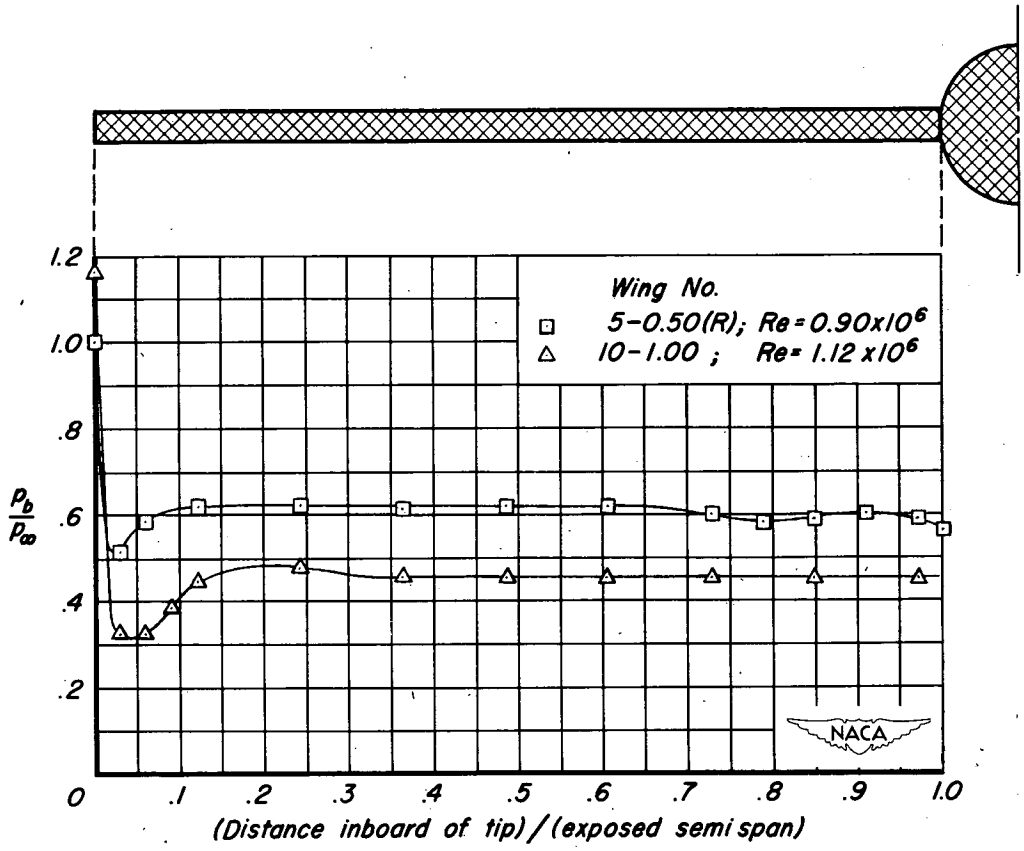

Figure 12.- Spanwise variation of base pressure for laminar boundary-layer flow; $M_\infty = 1.5$.

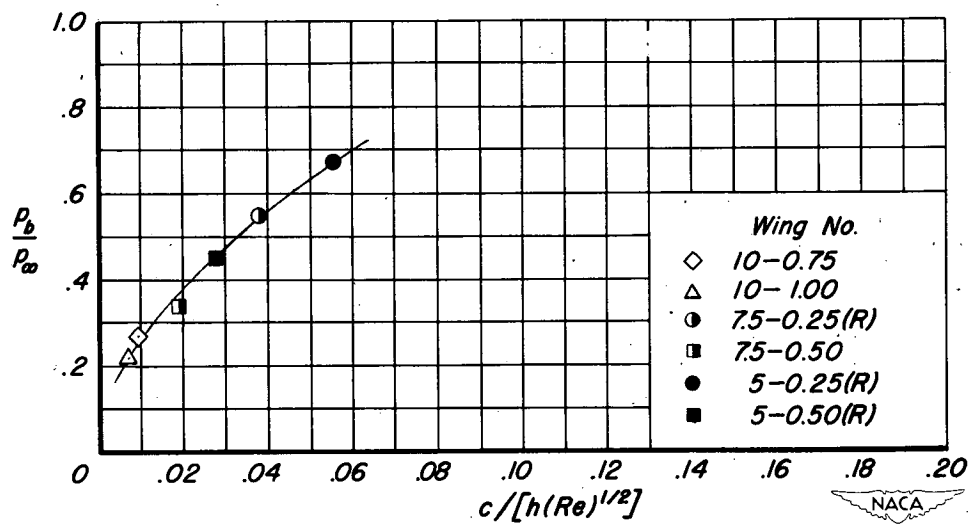

Figure 13.- Base pressure measurements on wings of the thickness group with laminar flow; $M_\infty = 3.1$, $Re = 2.0 \times 10^6$.

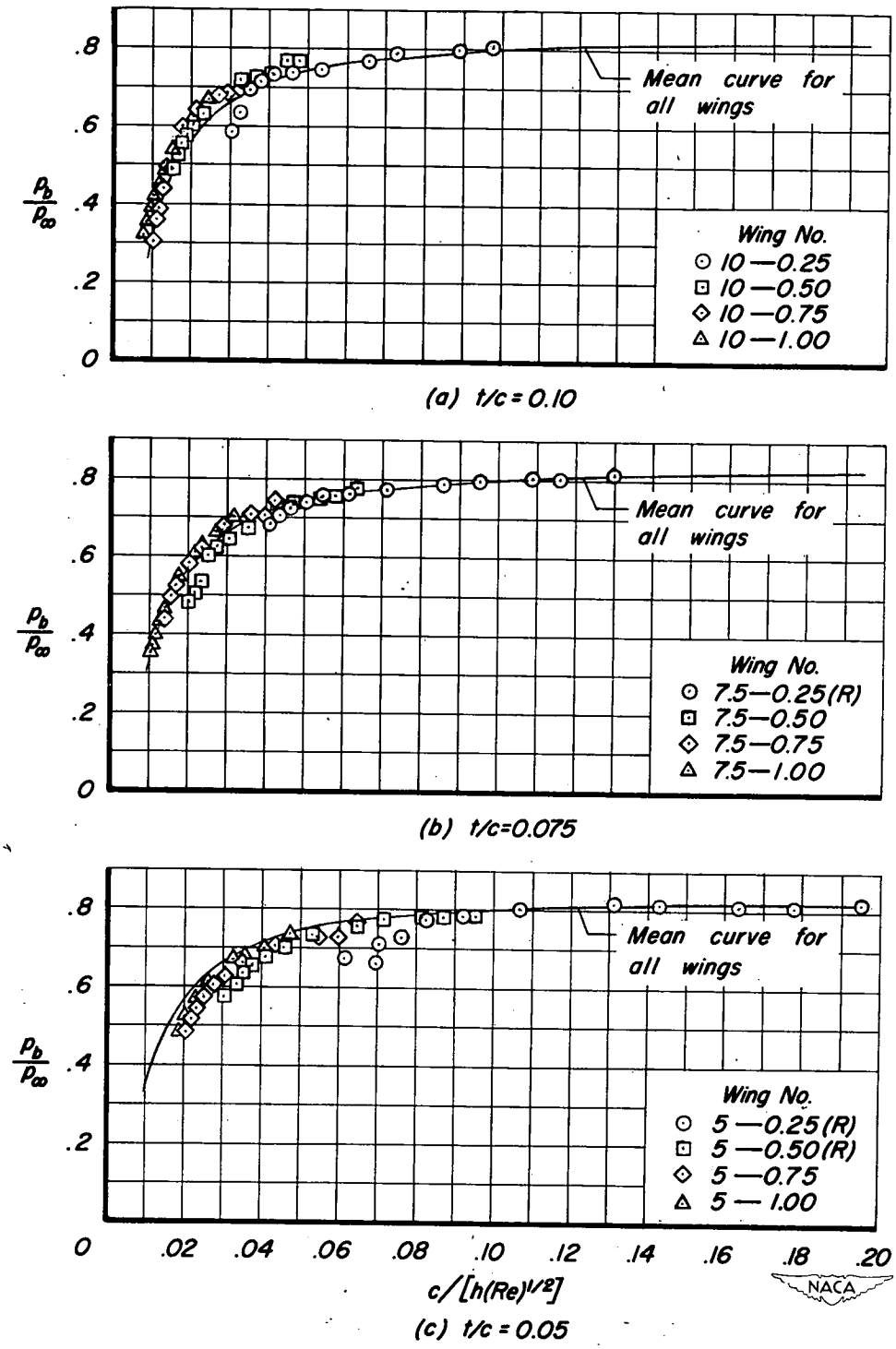

Figure 14.—Base pressure measurements on the thickness group of wings with laminar flow; M_∞=2.0.

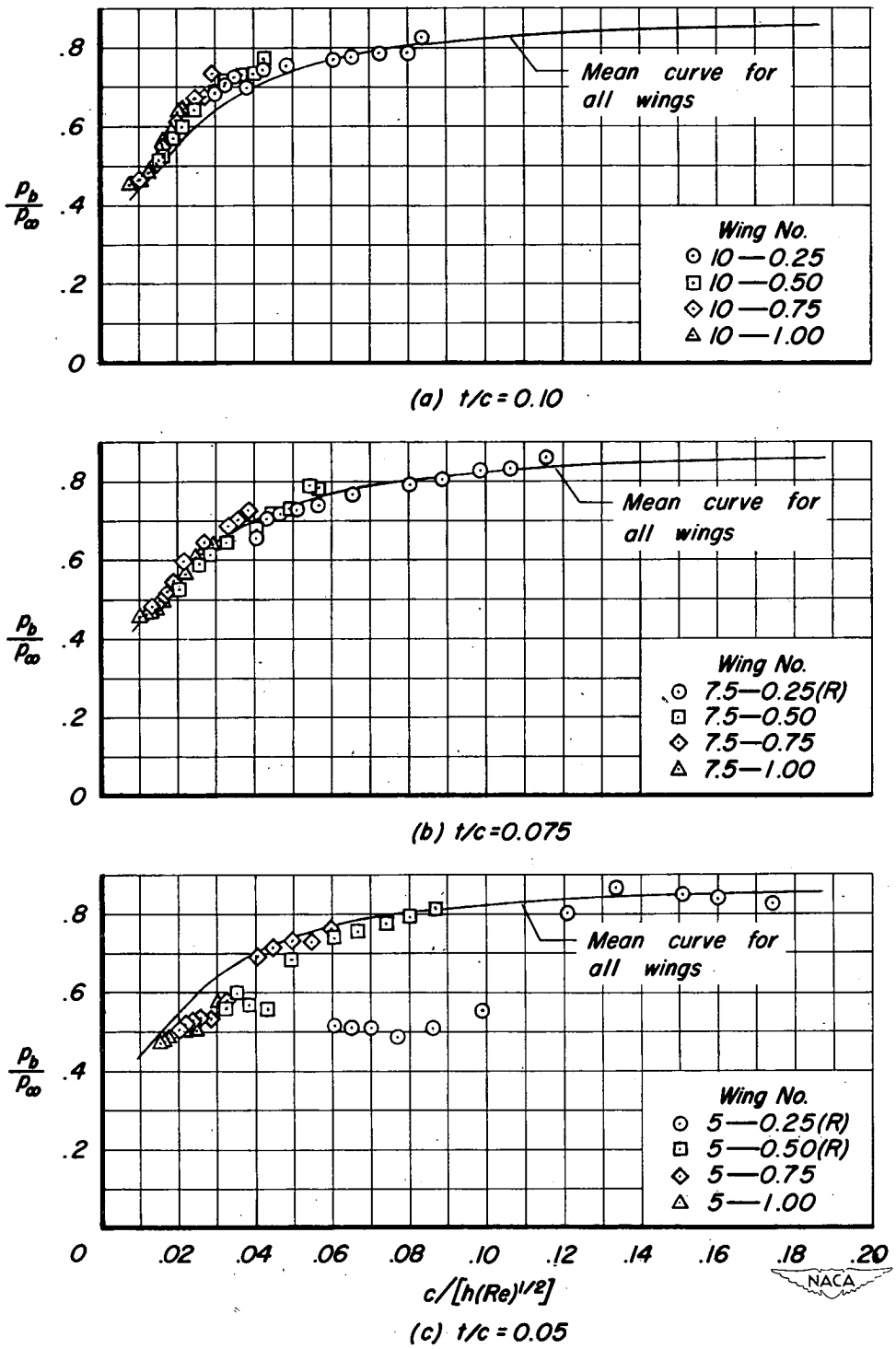

Figure 15.—Base pressure measurements on the thickness group of wings with laminar flow; M_∞=1.5.

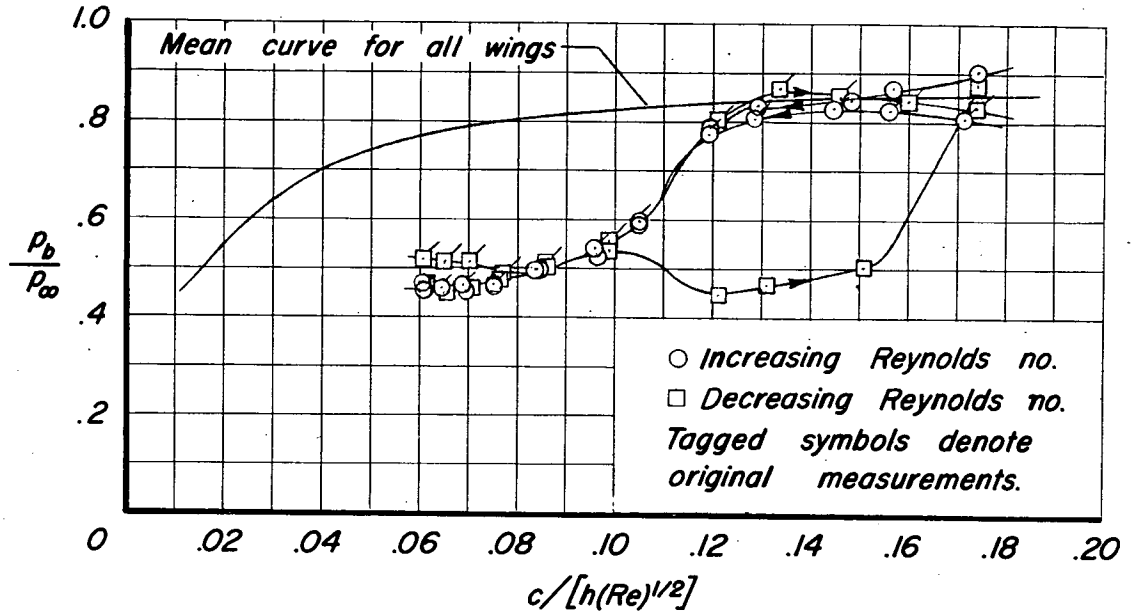

(a) Wing No. 5—0.25(R)

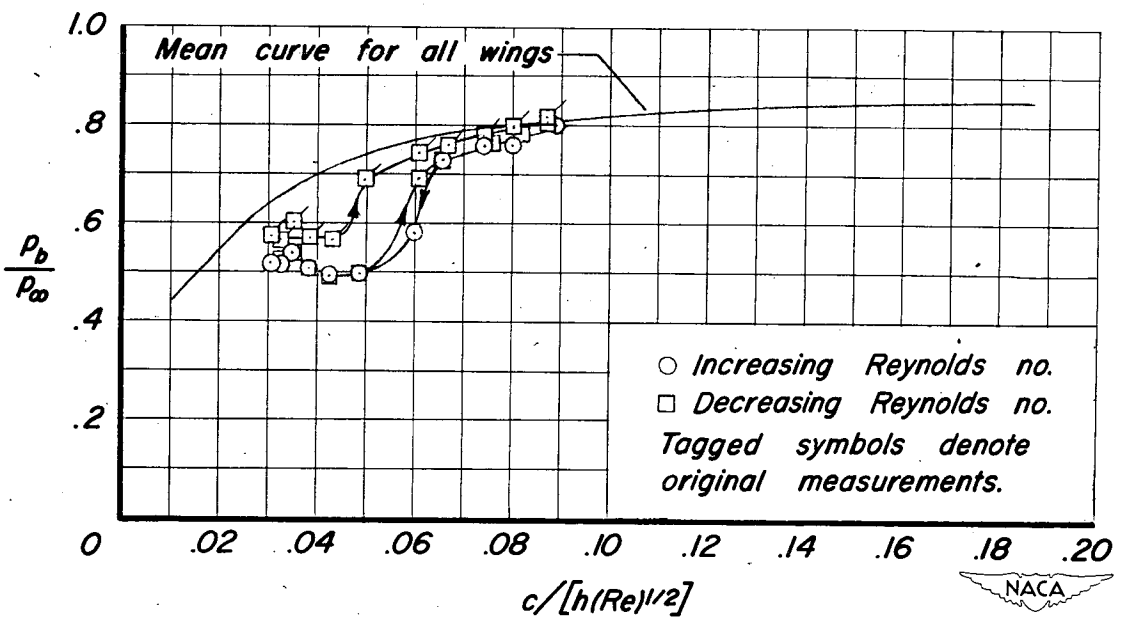

(b) Wing No. 5—0.50(R)

Figure 16.—Supplementary base pressure measurements on two 5-percent-thick wings at $M_\infty = 1.5$.

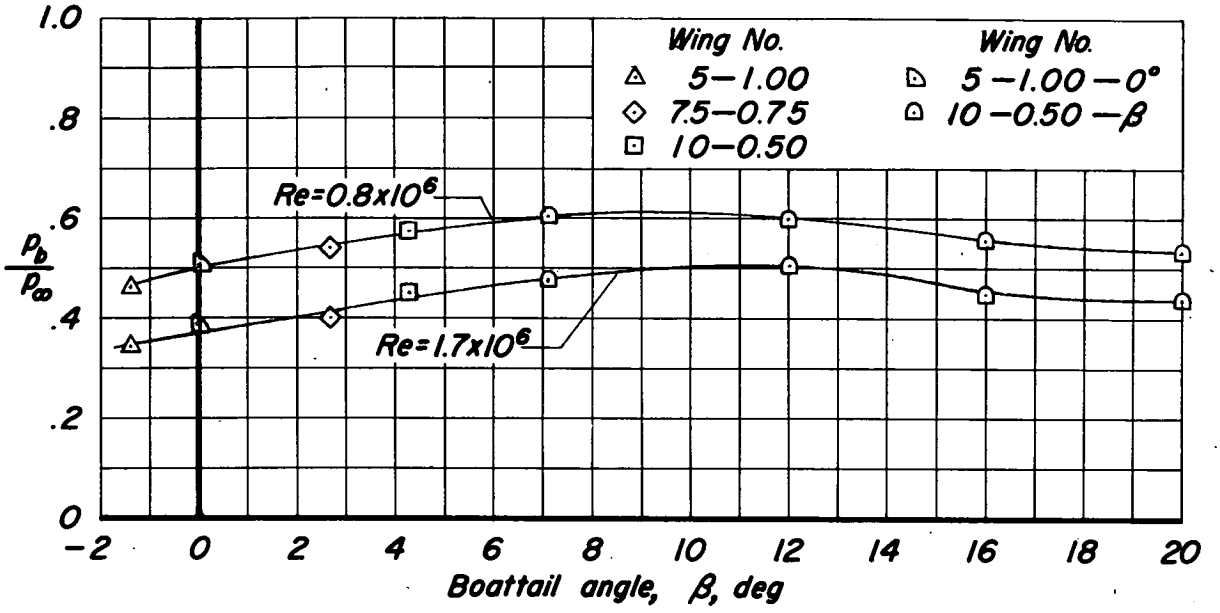

(a) M_∞=2.0; h/c=0.05

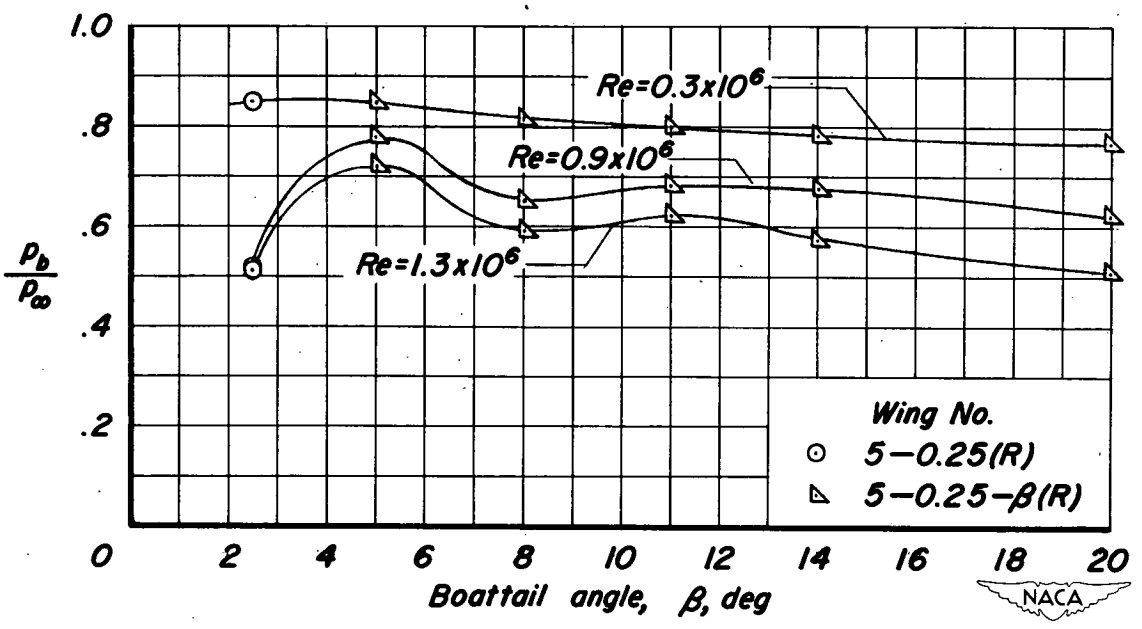

(b) M_∞=1.5; h/c=0.0125

Figure 17.—Effect of boattail angle on base pressure with laminar flow.

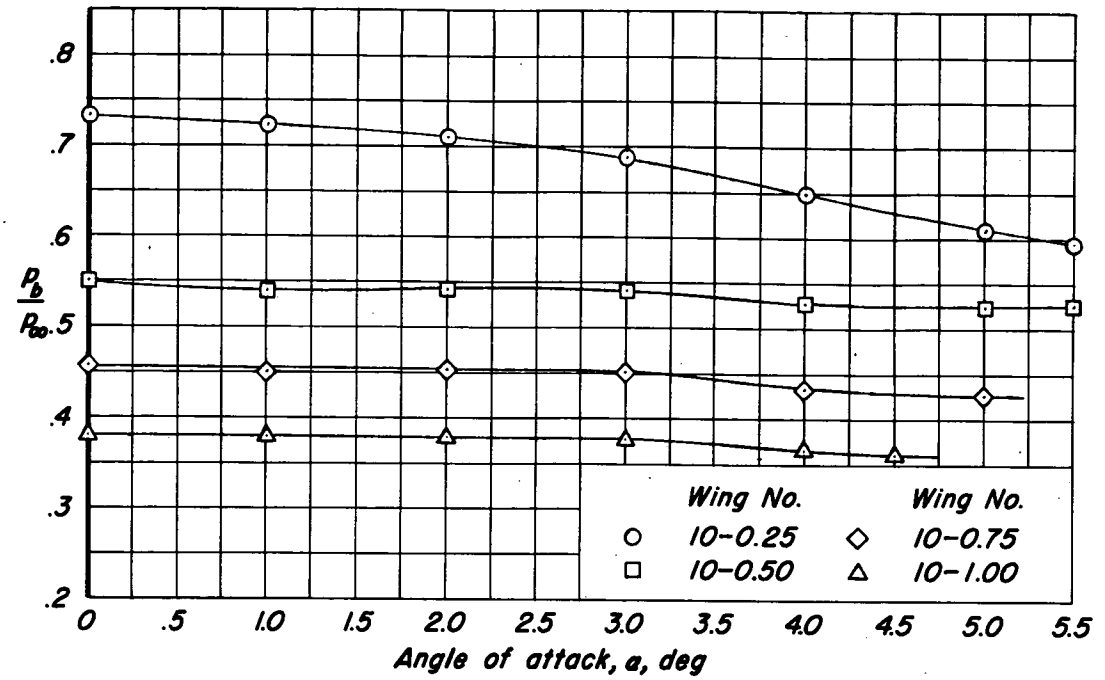

(a) t/c = 0.10

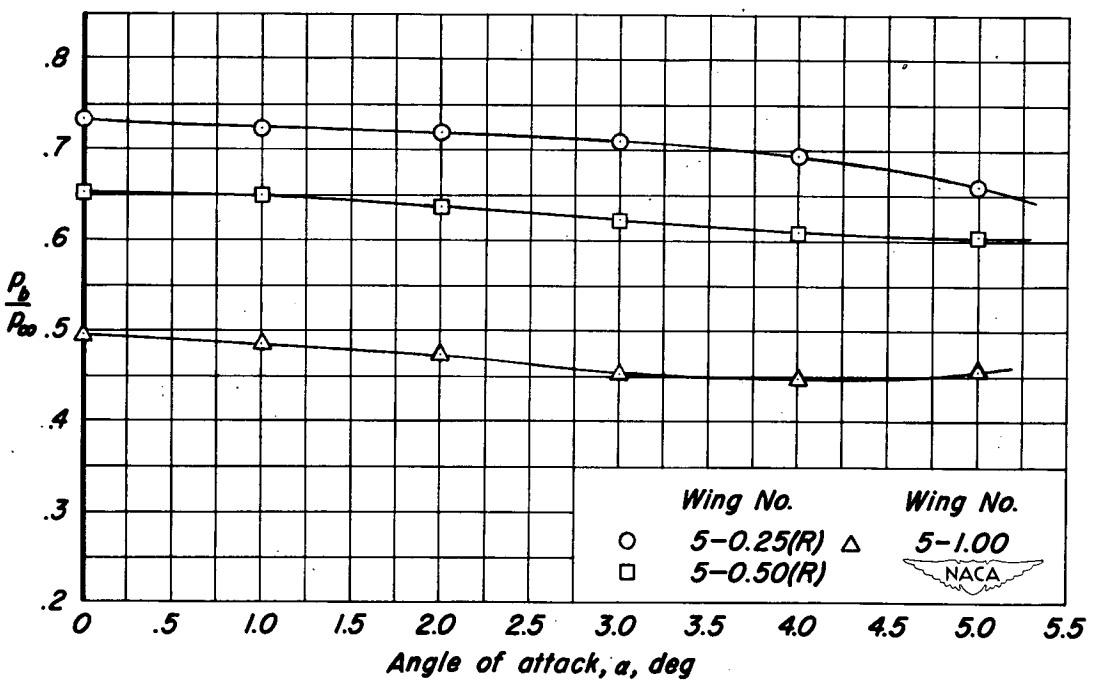

(b) t/c = 0.05

Figure 18. – Effect of angle of attack on base pressure for wings of the thickness group with laminar flow; M_∞=2.0, Re=1.0x10^6.

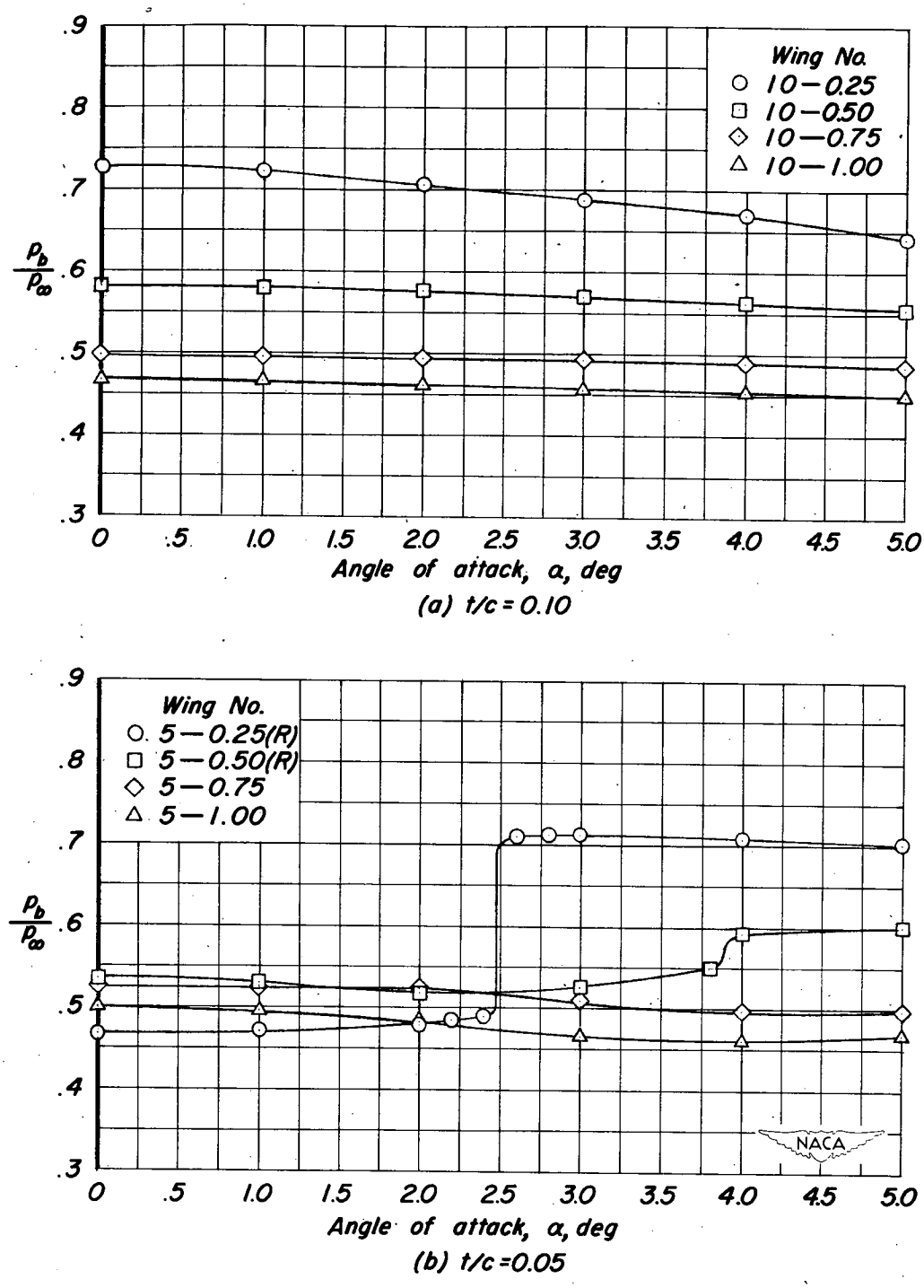

Figure 19.– Effect of angle of attack on base pressure for wings of the thickness group with laminar flow; M_∞=1.5, Re=1.1x10^6

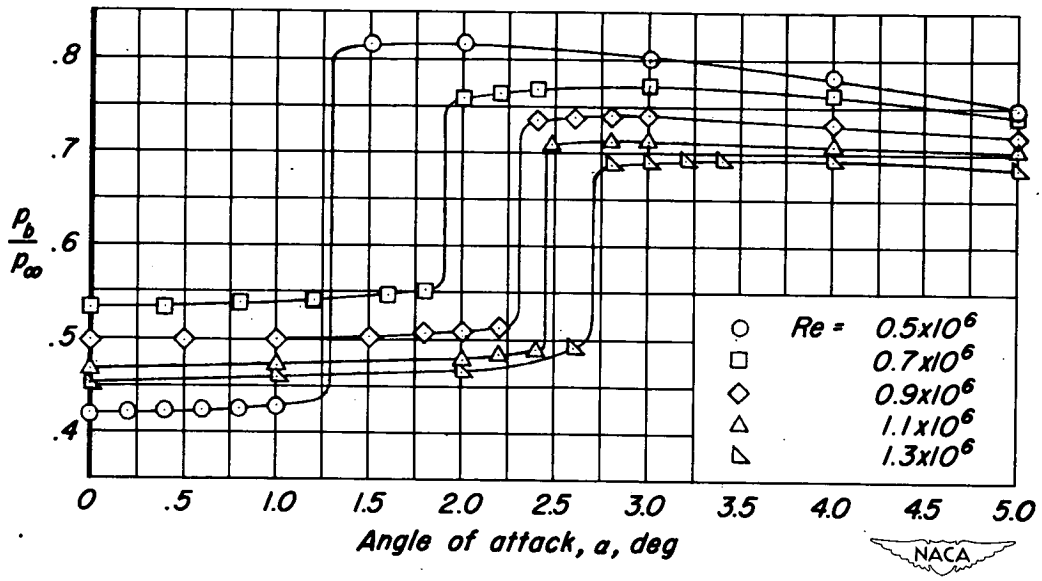

Figure 20.– Effect of angle of attack on base pressure for wing 5-0.25(R) with laminar flow at different Reynolds numbers; M_∞=1.5.

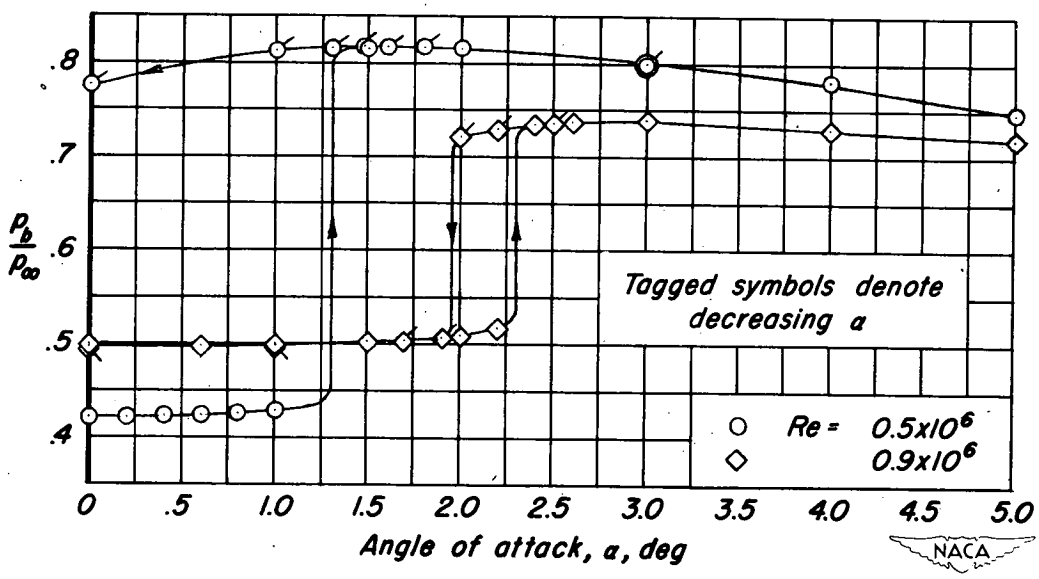

Figure 21. – Two types of hysteresis observed on wing 5-0.25(R) with laminar flow at M_∞=1.5.

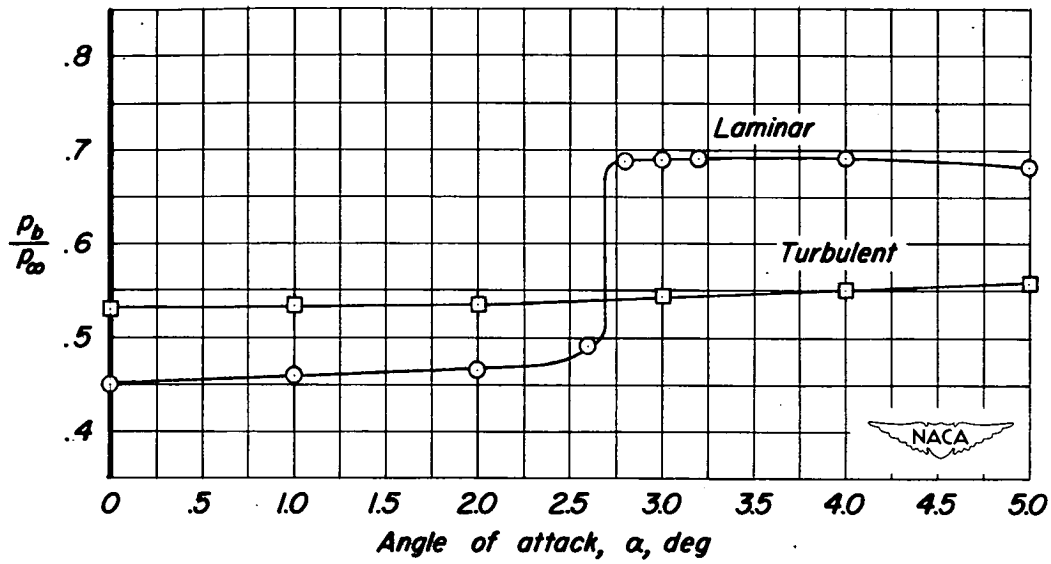

Figure 22.–Comparison of base pressure measurements on wing 5–0.25(R) with laminar and turbulent flow at M_∞=1.5, Re=1.3x10^6.

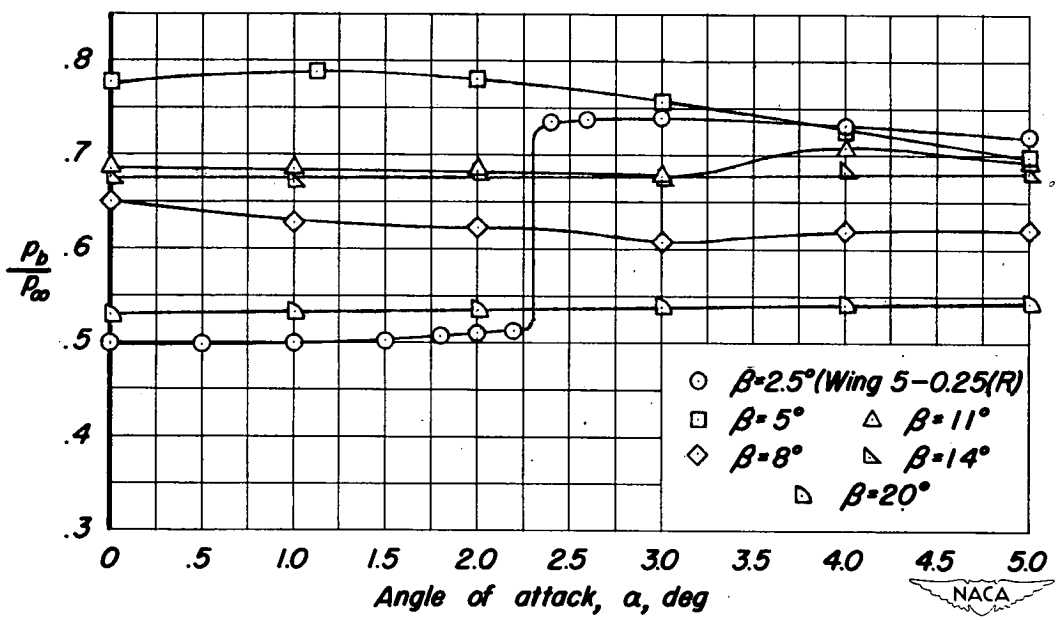

Figure 23.–Effect of angle of attack on the base pressure for 5-percent thick wings of the boattail group with laminar flow; M_∞=1.5, Re=0.9x10^6.

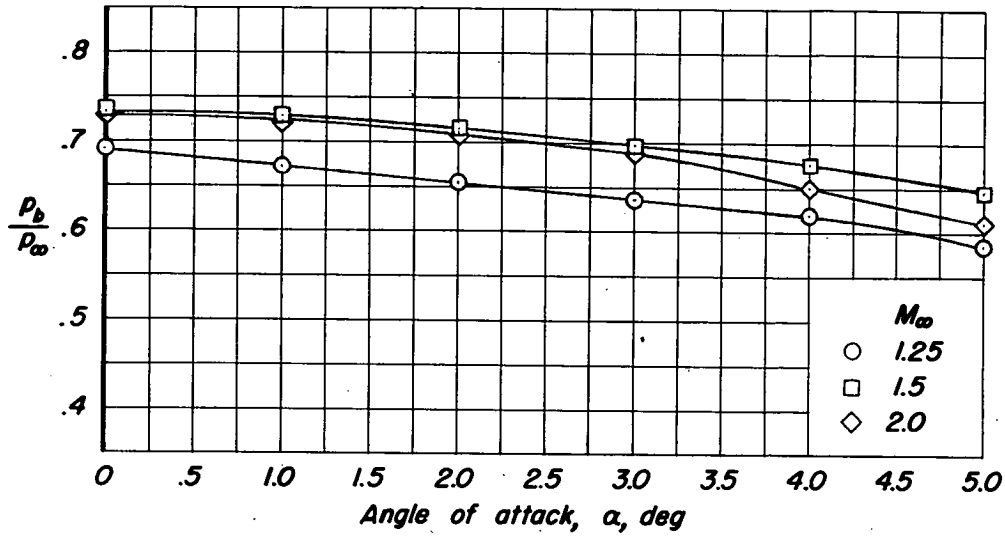

(a) Wing 10—0.25

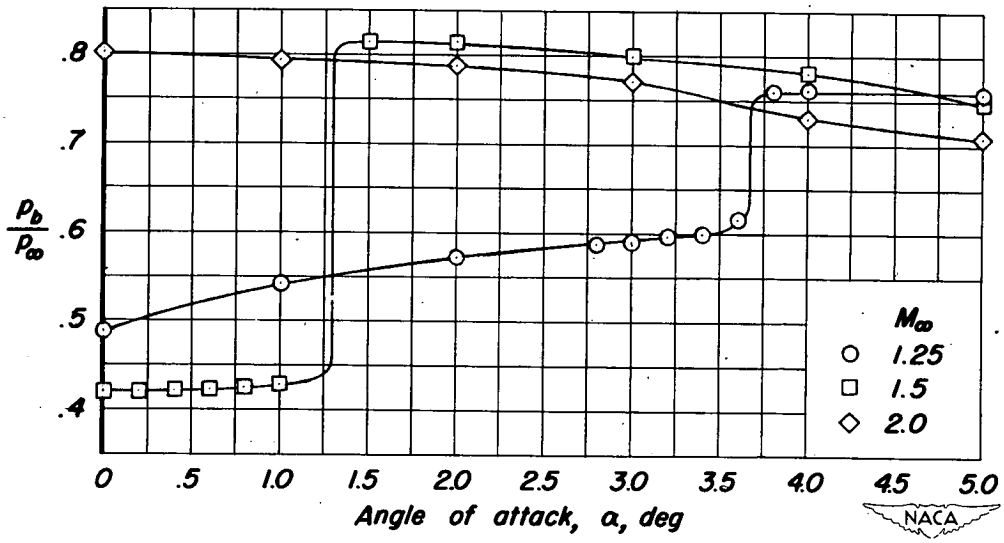

(b) Wing 5—0.25(R)

Figure 24.- Effect of angle of attack on base pressure at various Mach numbers for wings 10—0.25 and 5—0.25(R) with laminar flow; $Re = 0.5 \times 10^6$.

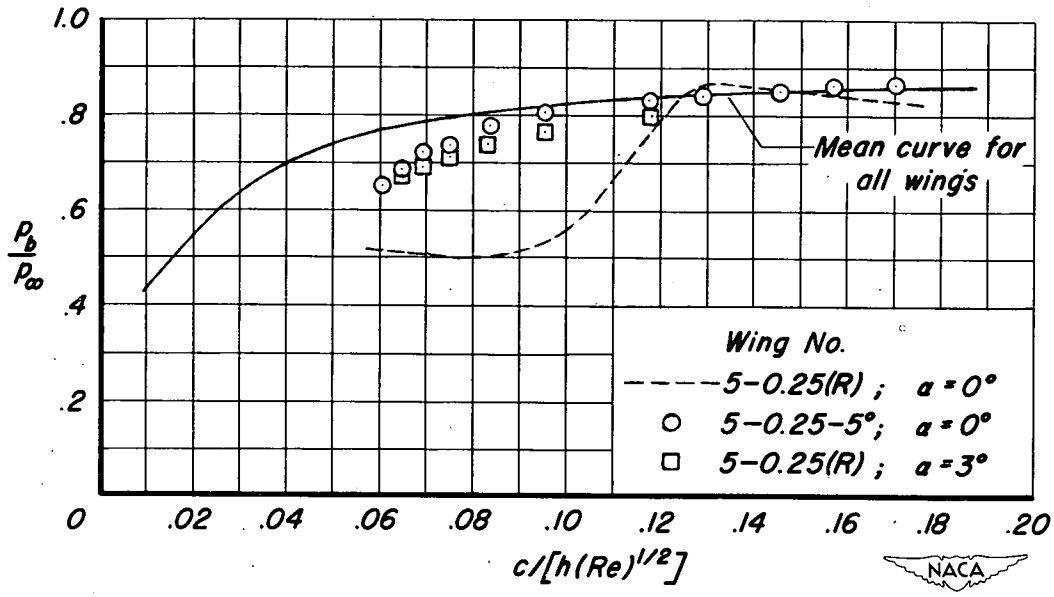

Figure 25.– Correlation of base pressure measurements on two 5-percent-thick wings at $M_\infty = 1.5$.

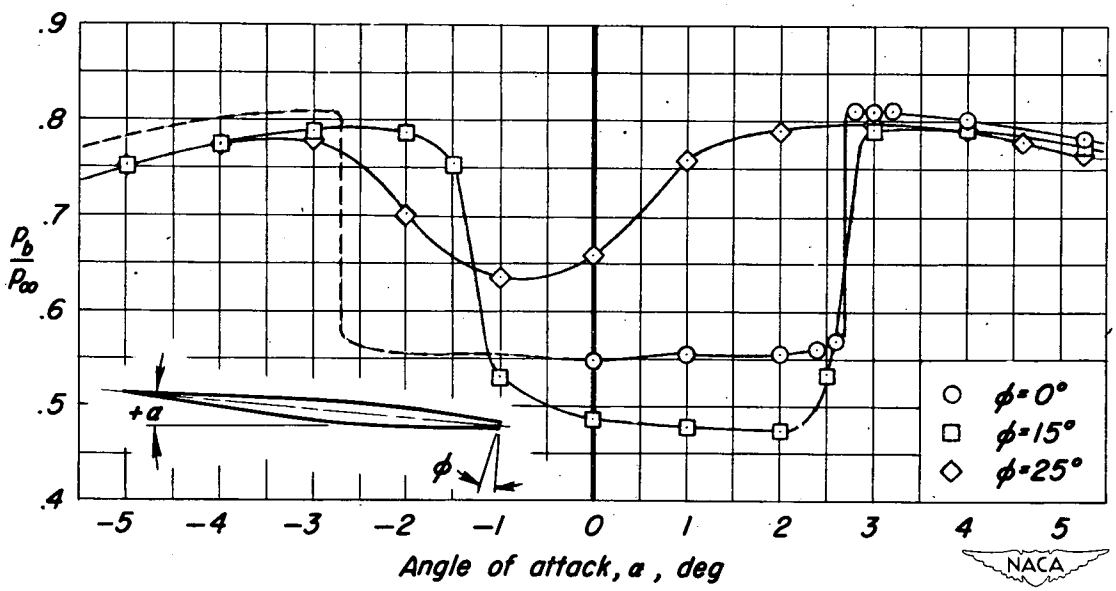

Figure 26.– Effect of bevel angle on base pressure for a wing with smooth surfaces tested at $M_\infty = 1.5$ and $Re = 0.5 \times 10^6$.

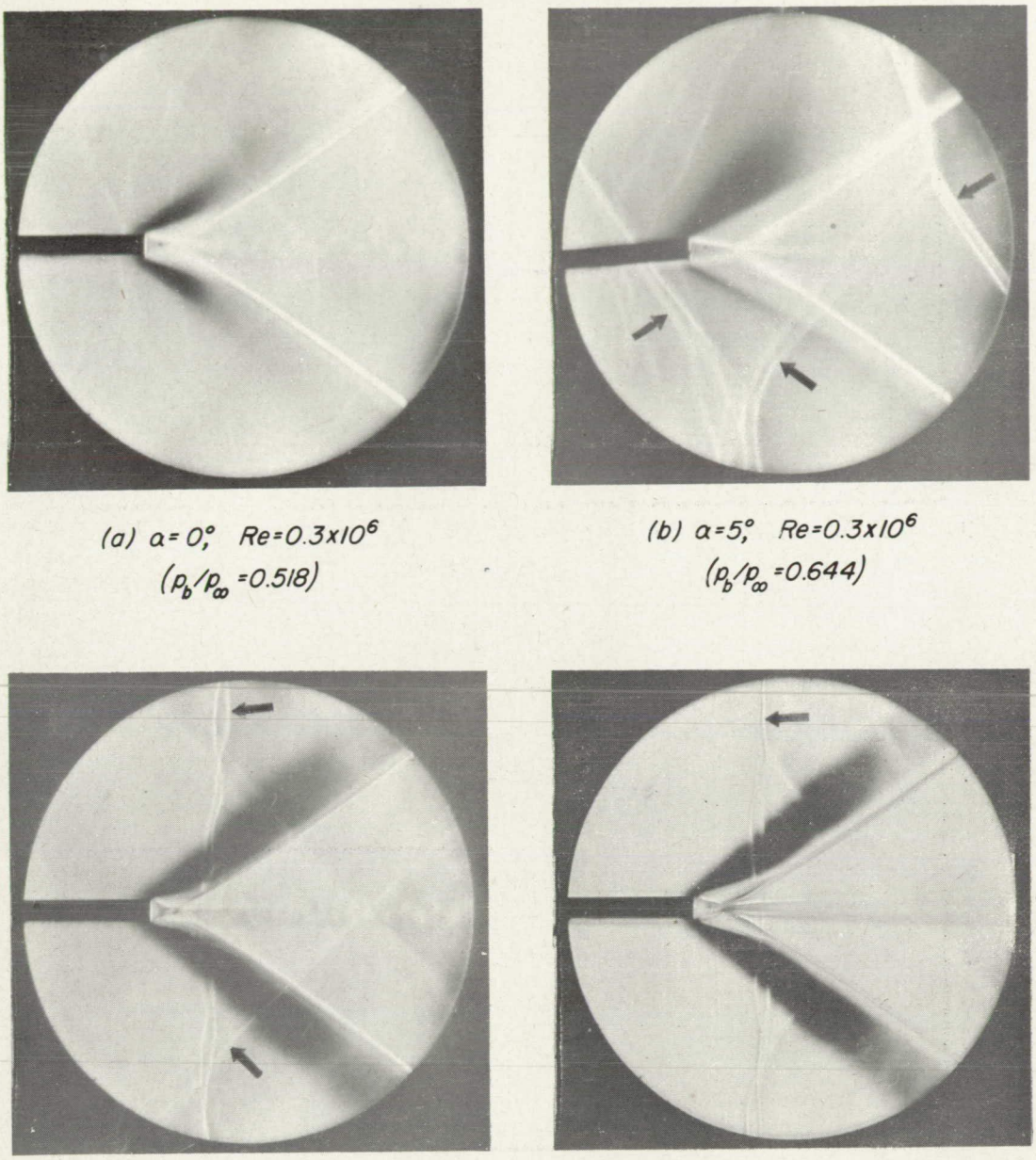

(a) $\alpha = 0°$, $Re = 0.3 \times 10^6$ ($p_b/p_\infty = 0.518$)

(b) $\alpha = 5°$, $Re = 0.3 \times 10^6$ ($p_b/p_\infty = 0.644$)

(c) $\alpha = 0°$, $Re = 1.2 \times 10^6$ ($p_b/p_\infty = 0.347$)

(d) $\alpha = 0°$, $Re = 2.0 \times 10^6$ ($p_b/p_\infty = 0.498$)

Note: Arrows point to disturbances existing between tunnel walls and boundary-layer plates. These disturbances are of no significance to the flow about the model.

Figure 27. – Typical schlieren photographs for a Mach number of 1.5.

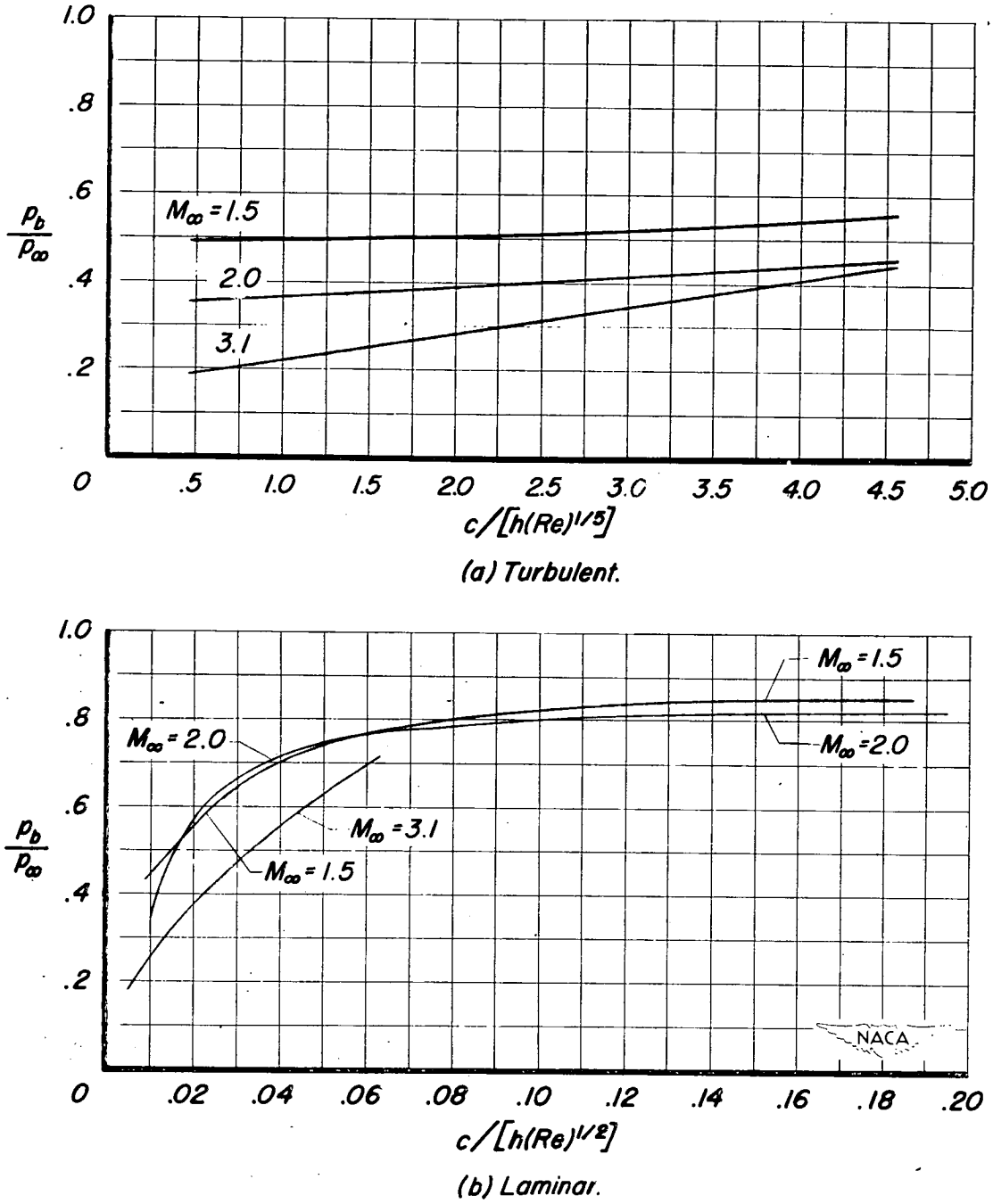

Figure 28.– Summary of faired curves representing average base pressure for all wings of the thickness group.

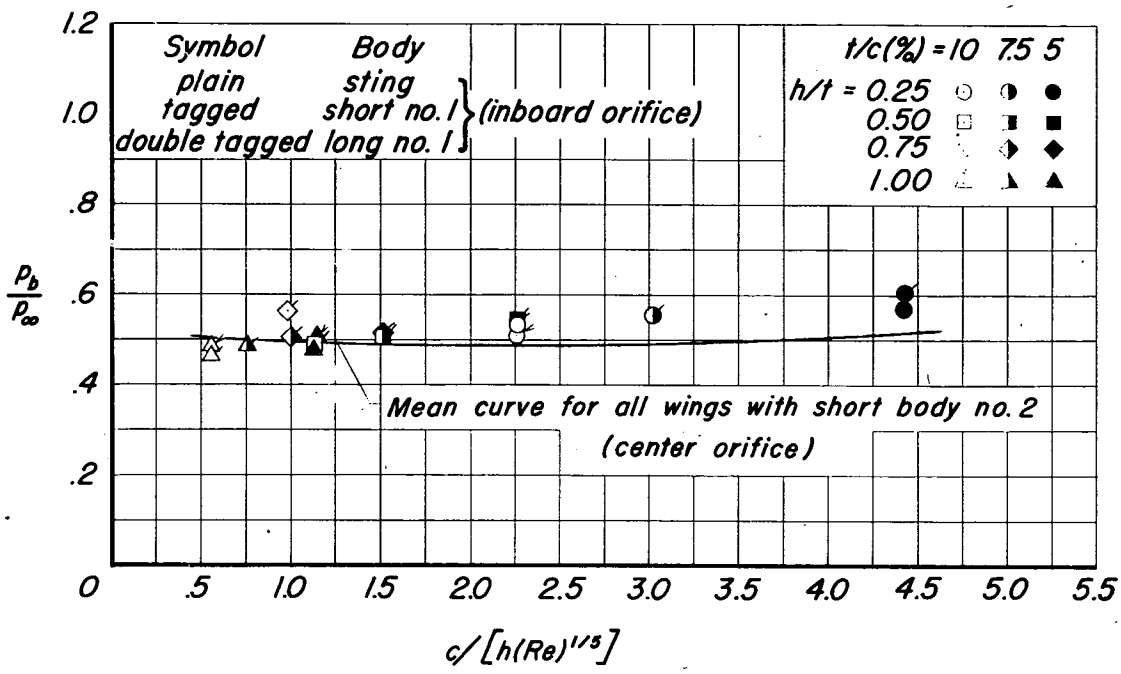

(a) $M_\infty = 1.5$

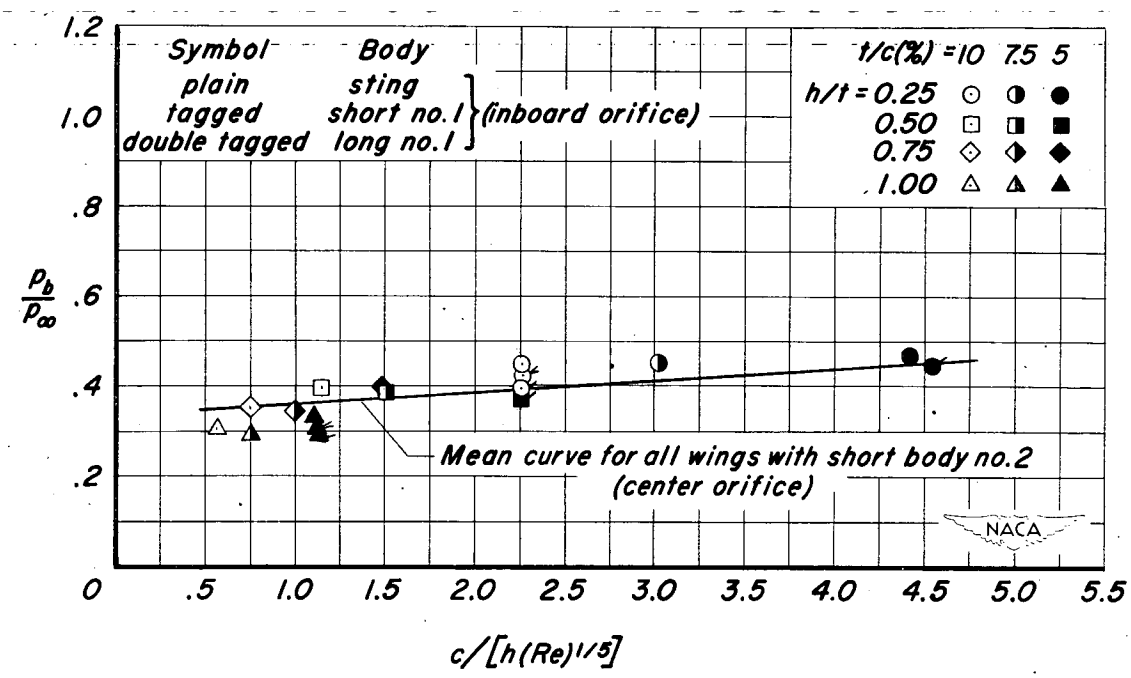

(b) $M_\infty = 2.0$

Figure 29. — The effect of different supports and orifice position on base pressure with turbulent flow.

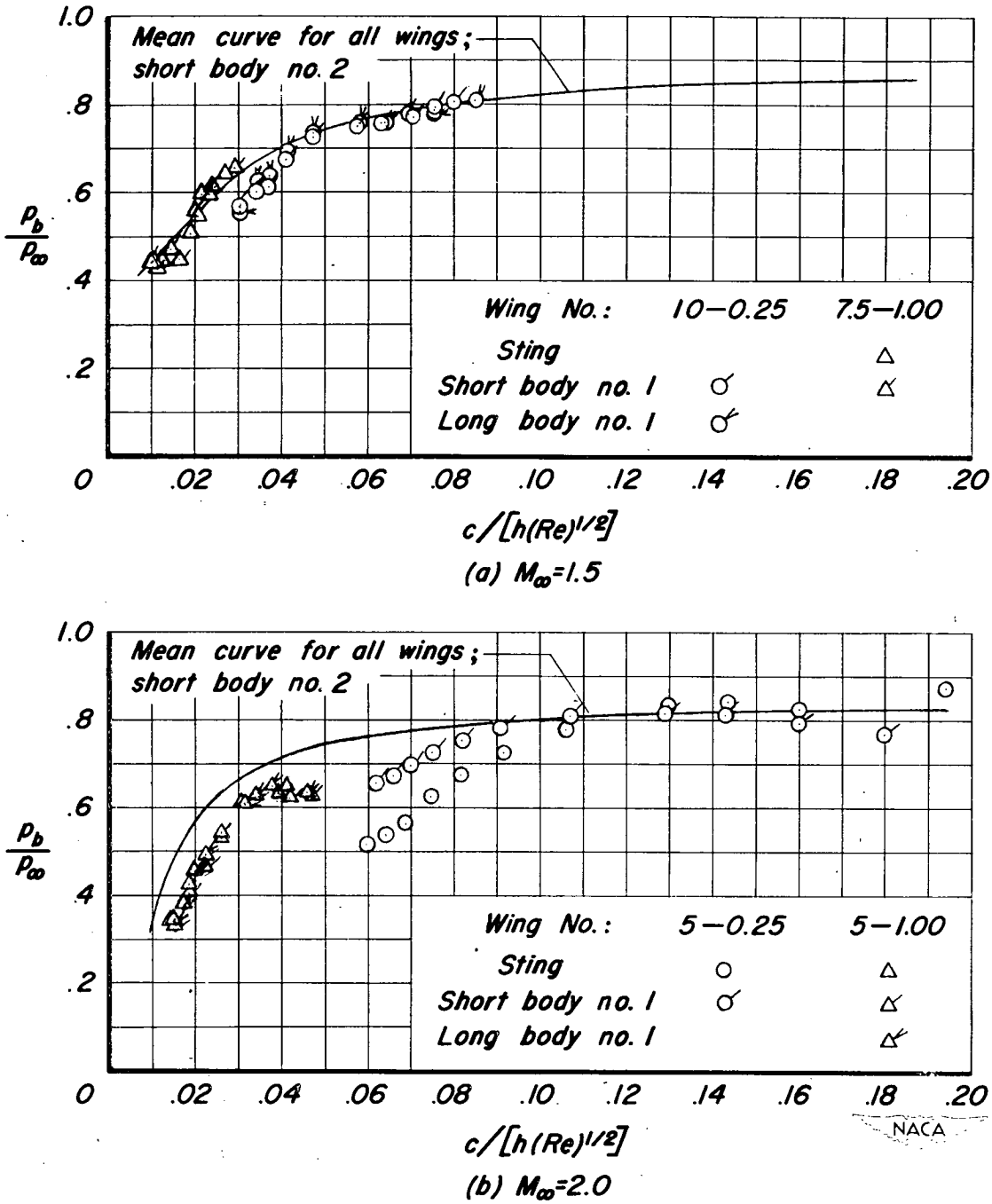

Figure 30.—Effect of different supports on base pressure with laminar flow.

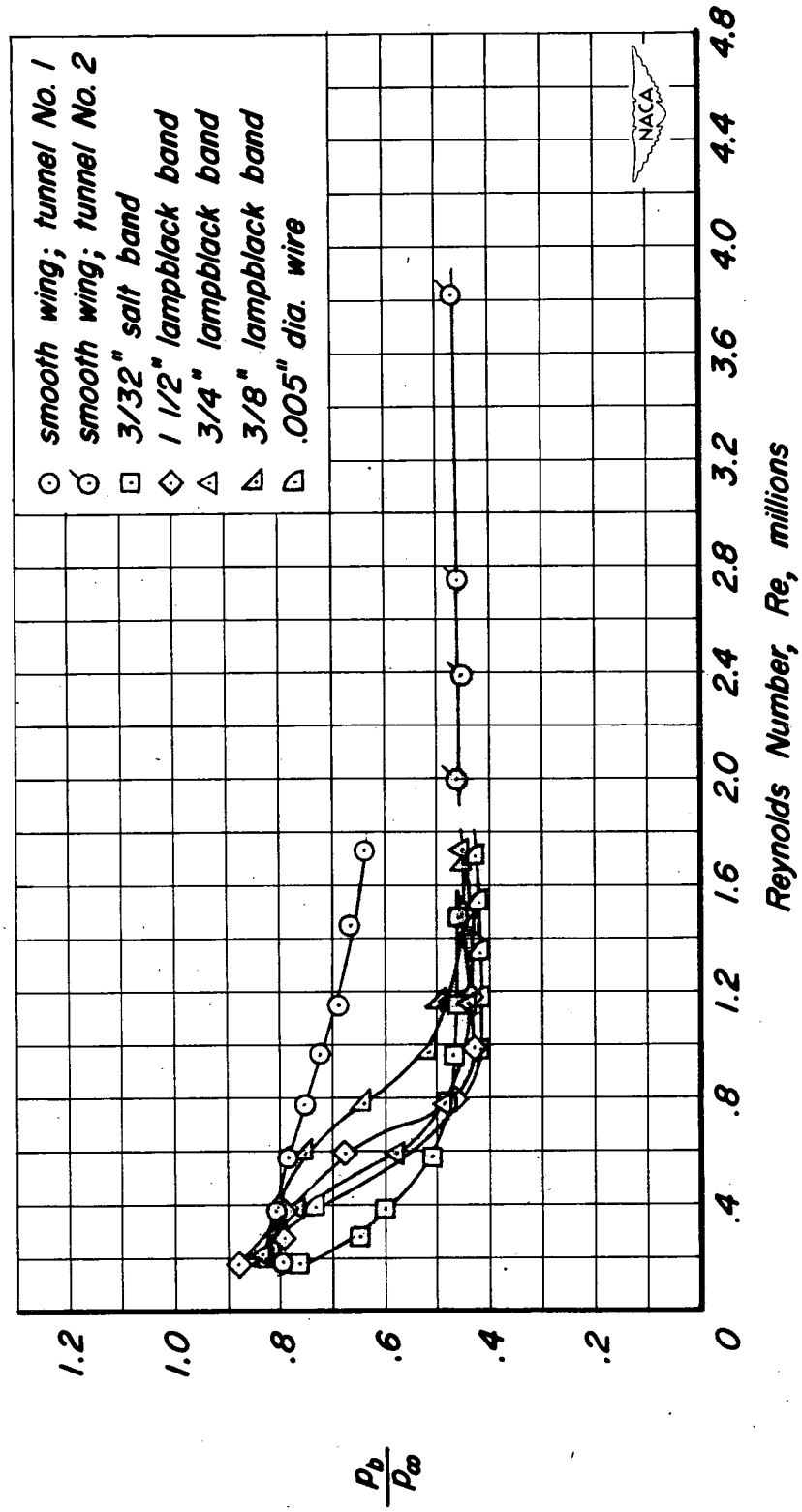

Figure 31. – The effect of the various boundary-layer trips on wing .10–0.25 at $M_\infty = 2.0$.